
Simulation of the laser plasma interaction with the PIC code **ALaDyn**

Carlo Benedetti

Department of Physics, University of Bologna & INFN/Bologna, ITALY

Overview of the presentation

1. Presentation of **ALaDyn**
2. Relevant **features** of **ALaDyn**
3. **Benchmarks** of the code
4. **Application I:** **ALaDyn** @ AO-FEL
5. **Application II:** **ALaDyn** @ PLASMONX
6. **Conclusions** and outlooks

1. Presentation of *ALaDyn*

1. Presentation of ALaDyn : general features

ALaDyn = Acceleration by Laser and Dynamics of charged particles

- born in 2007
- fully self-consistent, relativistic EM-PIC code
- “virtual-lab”: laser pulse(s) + injected bunch(es) + plasma \Rightarrow defined by the user
- written in C/F90, parallelized with MPI, organized as a LIBRARY
- the (same) code works in 1D, 2D and 3D Cartesian geometry
- relevant features: low/high order schemes in space/time + moving window + stretched grid + boosted Lorentz frame + hierarchical particle sampling
- devel. & maintain. @ Dep. of Phys. - UniBo for the INFN-CNR PlasmonX collaboration

”ALaDyn -philosophy”: **IMPROVE** algorithms/numerical schemes to **REDUCE** computational requirements \Rightarrow run 2D/3D simulations in few hours/days on **SMALL CLUSTERS** (< 100 CPUs) with an **ACCEPTABLE** accuracy

1. Presentation of ALaDyn : basic equations

Maxwell Equations [ME]

Vlasov Equation [VE], $f_s (s = e, i, \dots)$

$$\begin{cases} \frac{\partial \mathbf{B}}{\partial t} = -c \nabla \times \mathbf{E} \\ \frac{\partial \mathbf{E}}{\partial t} = c \nabla \times \mathbf{B} - 4\pi \sum_s q_s \int \mathbf{v} f_s d\mathbf{p} \end{cases} \Leftrightarrow \frac{\partial f_s}{\partial t} + \mathbf{v} \cdot \frac{\partial f_s}{\partial \mathbf{r}} + q_s \left(\mathbf{E} + \frac{\mathbf{v}}{c} \times \mathbf{B} \right) \cdot \frac{\partial f_s}{\partial \mathbf{p}} = 0$$

$$\Rightarrow \nabla \cdot \mathbf{B}(t) = 0 \text{ if } \nabla \cdot \mathbf{B}(0) = 0$$

$$\Rightarrow \nabla \cdot \mathbf{E}(t) = 4\pi \rho(t) \text{ if } \nabla \cdot \mathbf{E}(0) = 4\pi \rho(0) \text{ and } \frac{\partial \rho}{\partial t} + \nabla \cdot \mathbf{J} = 0$$

- fields $\mathbf{E}, \mathbf{B}, \mathbf{J}$ \rightarrow discretized on a grid with $N_x \times N_y \times N_z = 10^{7-8}$ points
- num. particles $(\mathbf{r}_i, \mathbf{p}_i)$ \rightarrow sample the phase space distribution ($\sim 10^{8-9}$ particles):

$$q_s f_s(\mathbf{r}, \mathbf{p}, t) \rightarrow C_{Np} \sum_i^{N_p^{(s)}} q_i^{(s)} \delta(\mathbf{r} - \mathbf{r}_i^{(s)}(t)) \delta(\mathbf{p} - \mathbf{p}_i^{(s)}(t))$$

$$VE[f_s] \Rightarrow \begin{cases} \frac{d\mathbf{r}_i^{(s)}}{dt} = \mathbf{v}_i^{(s)} \\ \frac{d\mathbf{p}_i^{(s)}}{dt} = q_i^{(s)} \left(\mathbf{E}(\mathbf{r}_i^{(s)}) + \frac{\mathbf{v}_i^{(s)}}{c} \times \mathbf{B}(\mathbf{r}_i^{(s)}) \right) \end{cases} \quad i = 1, 2, \dots, N_p^{(s)}$$

2. Relevant features of ALaDyn

2. Relevant features of ALaDyn : high order schemes[†]

- Spatial derivatives in the ME \Rightarrow **(compact) high order schemes**[†]

Denoting by f_i/f'_i the function/derivative on the i - th grid point

$$\alpha f'_{i-1} + f'_i + \alpha f'_{i+1} = a \frac{f_{i+1} - f_{i-1}}{2h} + b \frac{f_{i+2} - f_{i-2}}{4h} + c \frac{f_{i+3} - f_{i-3}}{6h} \quad (*)$$

\Rightarrow relation between a, b, c and α by matching the Taylor expansion of (*)

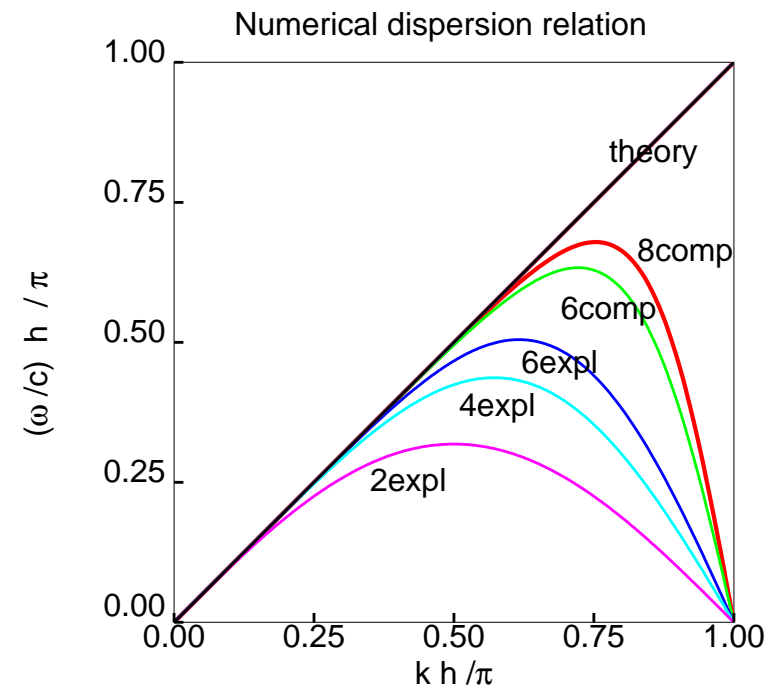
\Rightarrow if $\alpha \neq 0$, f'_i obtained by solving a **tri-diagonal** linear system

\Rightarrow “classical” 2^{nd} order: $\alpha = b = c = 0$, $a = 1$

1. improvement in the spectral accuracy

$\omega = \omega(k) \Rightarrow$

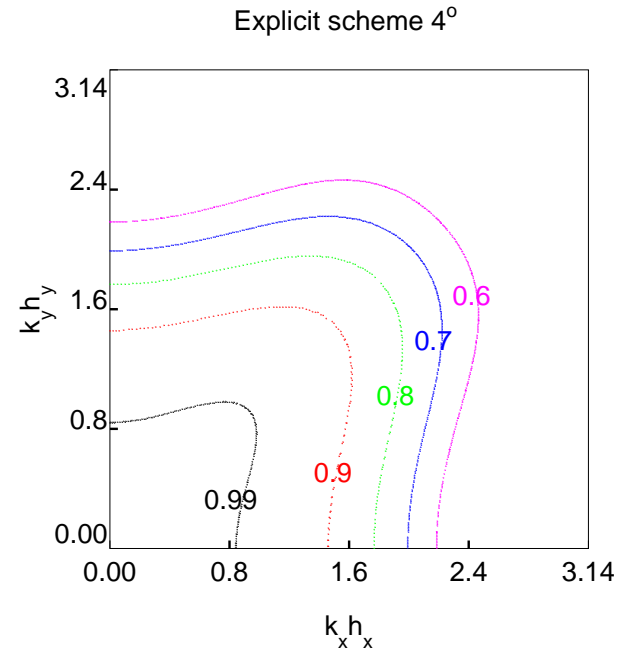
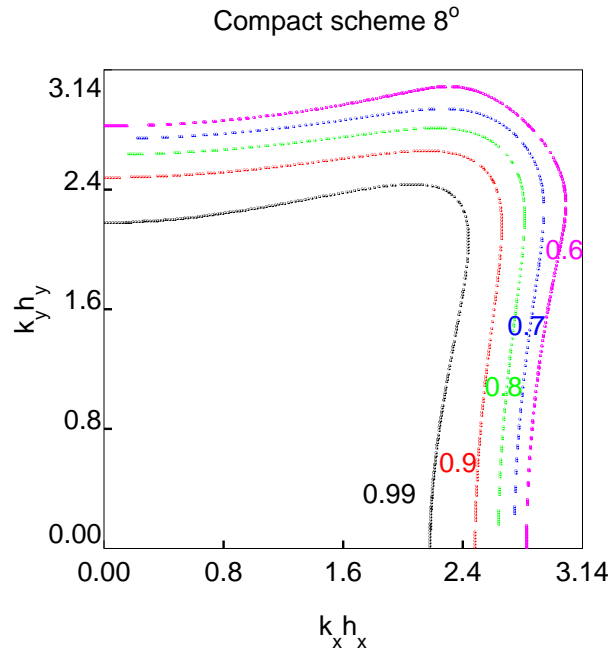
even with **few** (10-12) points/wavelength
the wave phase velocity is well reproduced



[†] S.K. Lele, JCP **103**, 16 (1992)

2. Relevant features of ALaDyn : high order schemes

2. improvement in the isotropy



- Time integration in the ME & particle Eq. of motion: high accuracy in the spatial derivatives requires high order time integration \Rightarrow **4th order Runge-Kutta scheme**

\Rightarrow With **high order schemes** we can adopt, for a given accuracy, a **coarser computational grid** allowing to use a **higher particles per cell number** and a **larger time step** compared to standard PIC codes (factor 3-10 gain). \Leftarrow

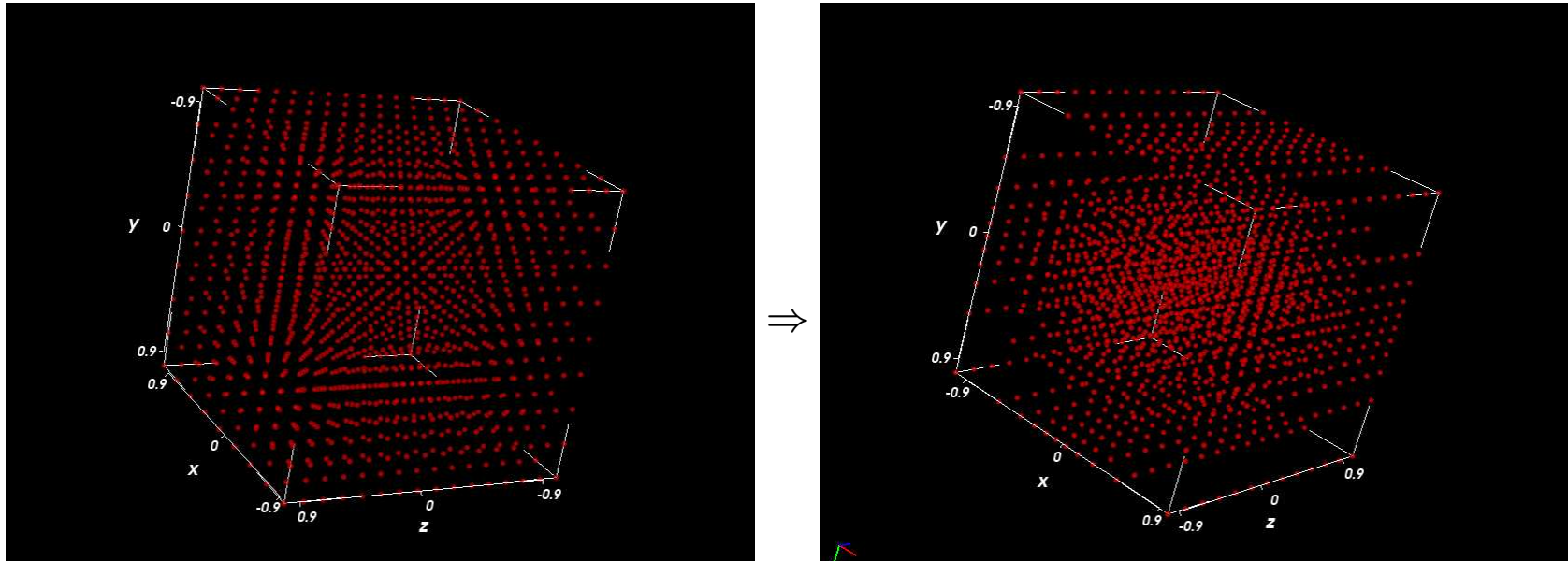
2. Relevant features of ALaDyn : stretched grid

- Stretched grid: **high accuracy in the centre** (sub- μm resolution in transv. plane) VS low accuracy in the borders (not interesting!)

$x_i \rightarrow$ “physical” transv. coordinate / $\xi_i \rightarrow$ “rescaled” transv. coordinate

$$x_i = \alpha_x \tan \xi_i, \quad \xi_i \text{ unif. distributed}$$

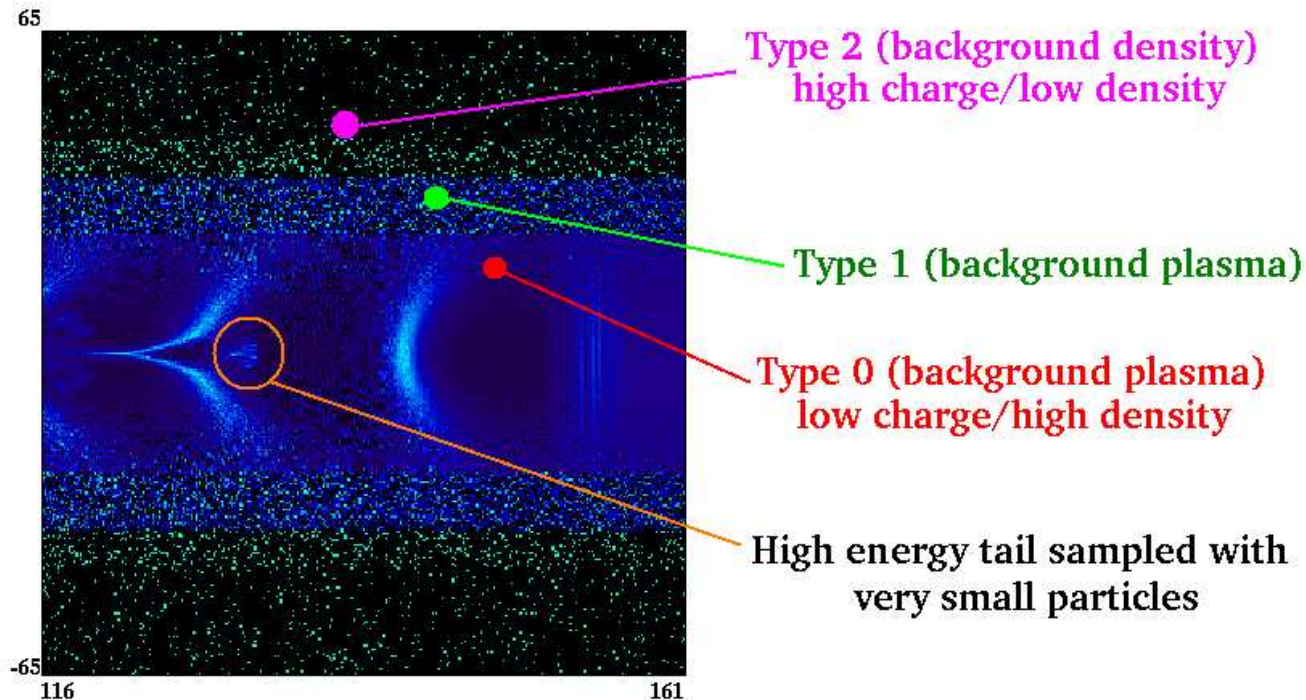
$\alpha_x \rightarrow$ “*stretching parameter*” ($\alpha_x \rightarrow \infty$ unif. grid, $\alpha_x \rightarrow 0$ super-stretched grid)



\Rightarrow Adopting a **transverse stretched grid** we (considerably) **reduce the number of grid points** allowing to **save memory** (keeping fixed the accuracy) compared to an uniform grid (max. gain ~ 100). \Leftarrow

2. Relevant features of ALaDyn : hierarchical particle sampling

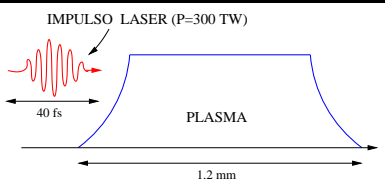
- A given particle species (*e.g.* electrons) can be sampled by a **family of macroparticles with different charge** putting more macroparticles in the physically interesting zones (center/high energy tails) and less in the borders...



⇒ We can **reduce the total number of particles** involved in the simulation (especially when the stretched grid is enabled) AND **decrease the statistical noise** (*i.e.* increase the reliability of the results). ⇐

2. Relevant features of ALaDyn : the Boosted Lorentz Frame

- The space/time scales spanned by a system are **not invariant** under Lorentz transform.[†]
 \Rightarrow the “computational complexity” can be reduced changing the reference system

Laboratory Frame	Boosted Lorentz Frame (β_*)	
$\lambda_0 \rightarrow$ laser wavelength $\ell \rightarrow$ laser length $L_p \rightarrow$ plasma length $c\Delta t < \Delta z \ll \lambda_0, \lambda_0 < \ell \ll L_p$ $\Rightarrow t_{simul} \sim (L_p + \ell)/c$ $\# \text{ steps} = \frac{t_{simul}}{\Delta t} \propto \frac{L_p}{\lambda_0} \gg 1$ large # of steps	$\lambda'_0 = \gamma_*(1 + \beta_*) \lambda_0 > \lambda_0$ $\ell' = \gamma_*(1 + \beta_*) \ell > \ell$ $L'_p = L_p/\gamma_* < L_p$ $\Rightarrow t'_{simul} \sim (L'_p + \ell')/(c(1 + \beta_*))$ $\# \text{ steps}' = \frac{t'_{simul}}{\Delta t'} \propto \frac{L_p}{\lambda_0 \gamma_*^2 (1 + \beta_*)^2}$ # of steps reduced ($1/\gamma_*^2$)	

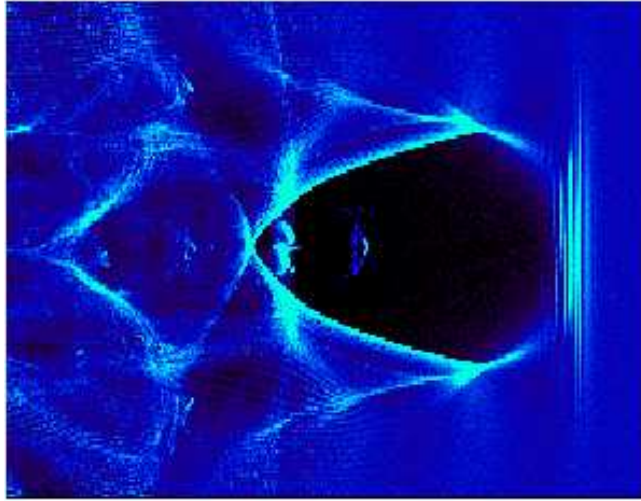
\Rightarrow diagnostics is more difficult ($t = \text{cost in the LF} \nRightarrow t' = \text{cost in the BLF}$)

\Rightarrow We can **reduce the simulation length** changing the reference system (useful for parameter scan). \Leftarrow

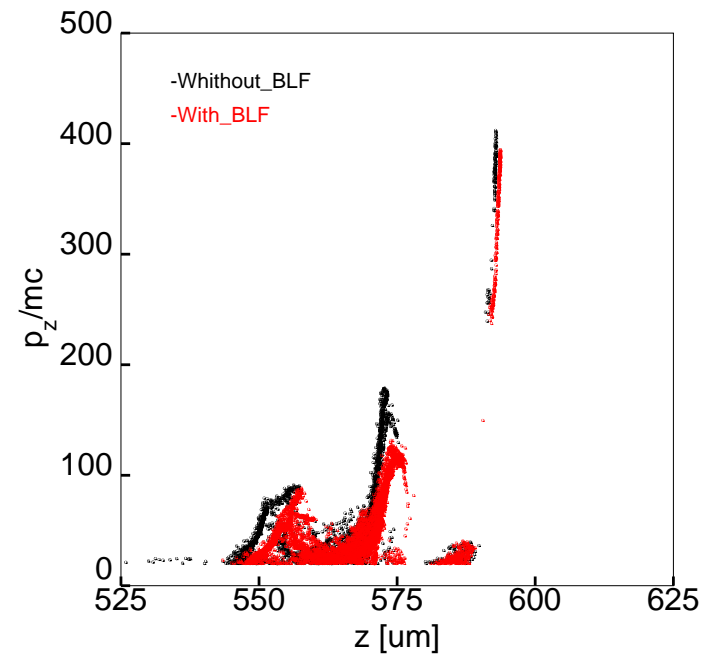
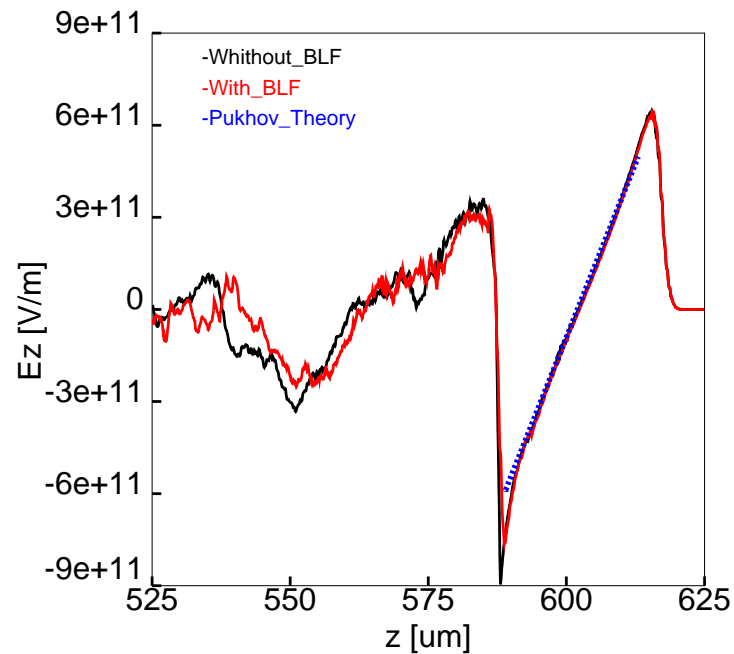
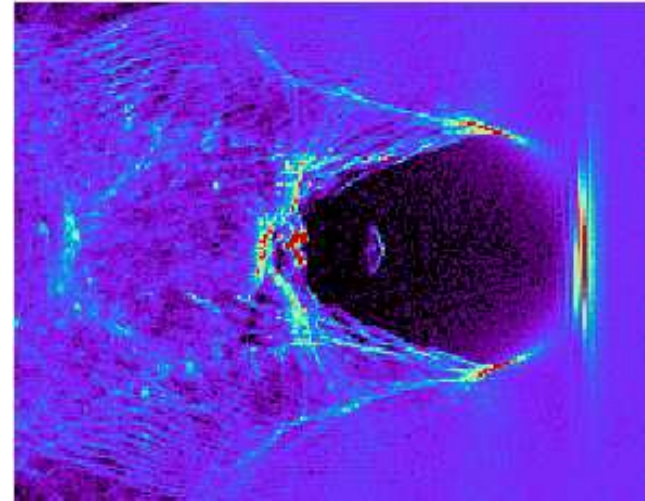
[†] J.L. Vay, PRL **98**, 130405 (2007)

2. Relevant features of ALaDyn : the Boosted Lorentz Frame

without BLF [t=46.3 h]



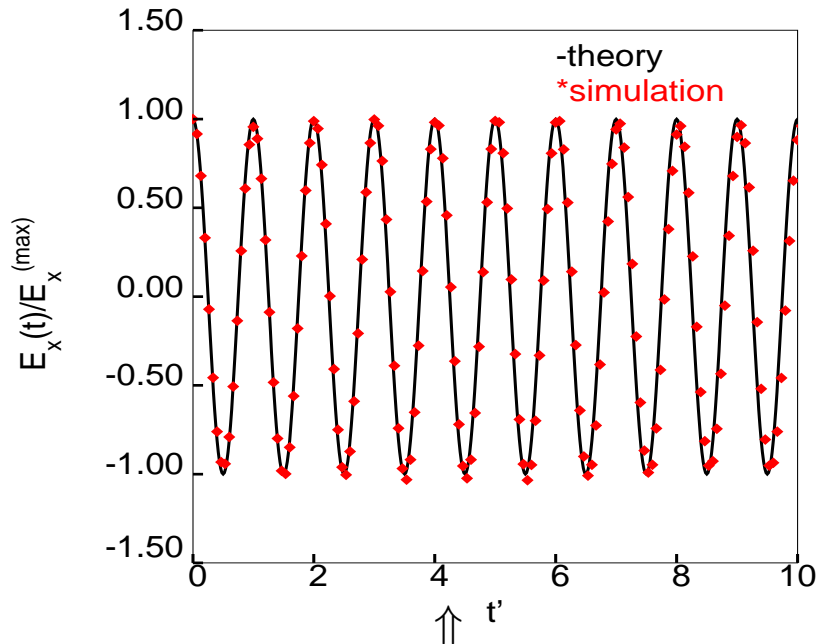
with BLF, $\beta_* = 0.9$ [t=8.1 h]



3. Benchmarks of the code

3. Benchmarks of the code: analytic solutions

- **ALaDyn** has been benchmarked against “standard” plasma physics problems



Plasma oscillation

- $\delta n/n_0 \sim 3\%$
- grid: 19 points
- 200 particles/cell
- $\Delta t = T_{plasma}/15$

$$\omega_P^{th} = 2.52 \cdot 10^{14} \text{ rad/s}$$

$$\omega_P^{si} = 2.51 \cdot 10^{14} \text{ rad/s}$$

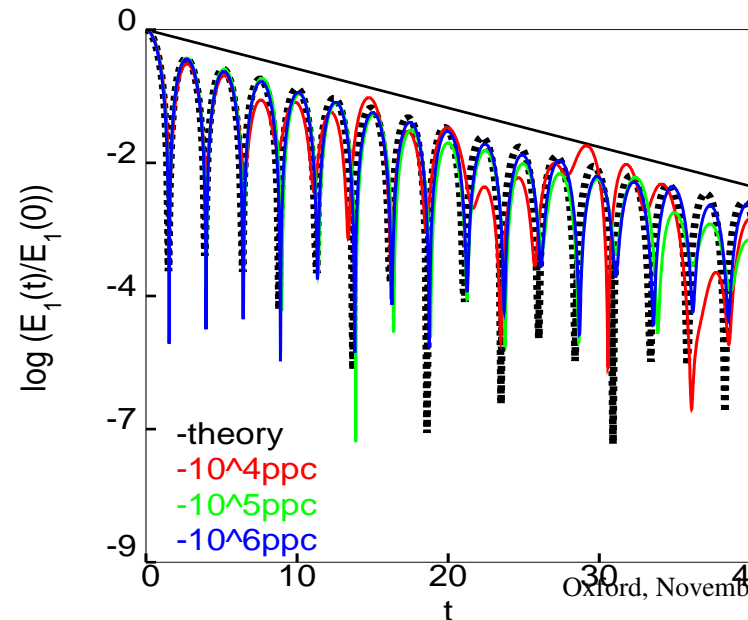
error < 0.4 %

Linear Landau damping

$$f_e = (1 + 0.02 \sin(kx)) \times \exp(-v^2/2)/\sqrt{2\pi}$$

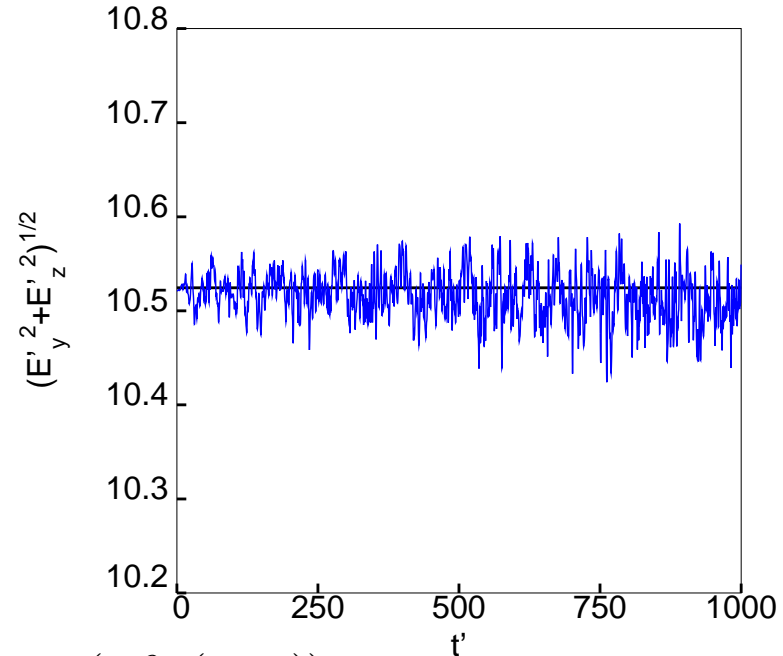
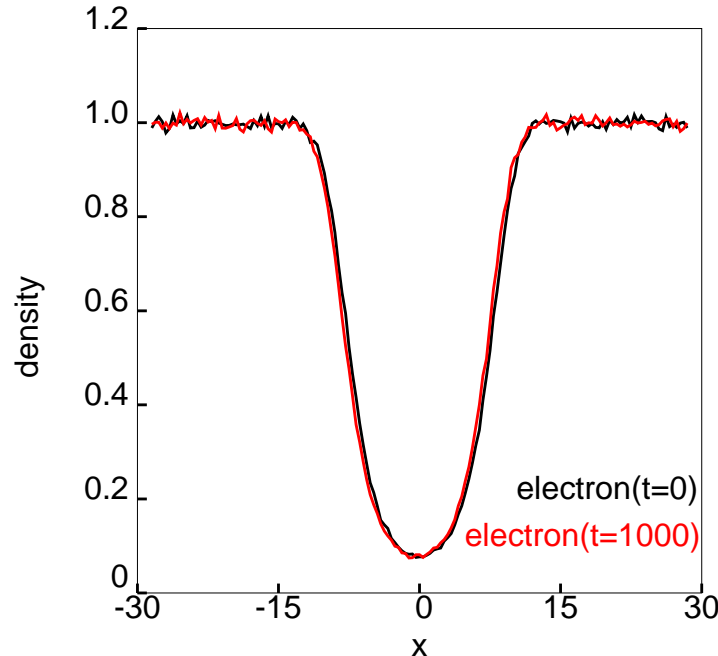
- grid: 16 points
- $10^4 - 10^6$ particles/cell

agreement with
Vlasov-fluid (512×1024)



3. Benchmarks of the code: analytic solutions

- 1D EM Solitons in a e^+/e^- overdense plasma + trapped radiation with CP ^a



⇒ Stationary solution of the VE: $f_{e+} = f_{e-} = \frac{\exp(-\beta \gamma(x, u_x))}{2K_1(\beta)}$ where $\gamma = \sqrt{1 + |a|^2 + u_x^2}$,

$a(x, t) = a_y(x, t) + i a_z(x, t) = a_0(x) \exp(i\omega t)$. The vector potential satisfies

$$\frac{d^2 a_0}{dz^2} + \omega^2 a_0 = 2a_0 \frac{K_0(\beta \sqrt{1+a_0^2})}{K_1(\beta)}, \quad \frac{1}{2} \omega^2 A_0^2 + \frac{2}{\beta} \left(\sqrt{1 + A_0^2} \frac{K_1(\beta \sqrt{1+A_0^2})}{K_1(\beta)} - 1 \right) = 0$$

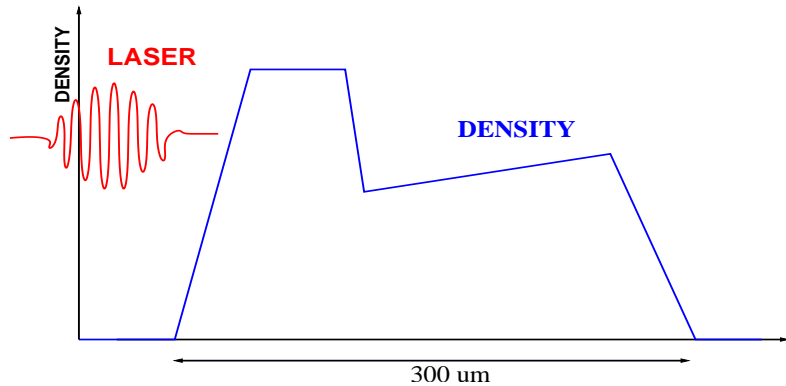
⇒ Simulation: grid with 150 points + 10^4 particles/cell

the soliton is stable

^aM. Lontano, *et. al*, Phys. Plas. **9**/6, 2562 (2002)

3. Benchmarks of the code: HO vs LO schemes

- Test based on the nonlinear **LWFA** regime:



Plasma:

- first plateau: $L_1 = 30 \mu m$, density 10^{19} e/cm^3
- accelerating plateau: $L_2 = 220 \mu m$

Laser:

- $\lambda_0 = 0.8 \mu m$, $P = 60 \text{ TW}$, $\tau_{FWHM} = 17 \text{ fs}$,
 $w_0 = 16 \mu m$

- **ALaDyn High Order** (3.8h on 4 CPUs)

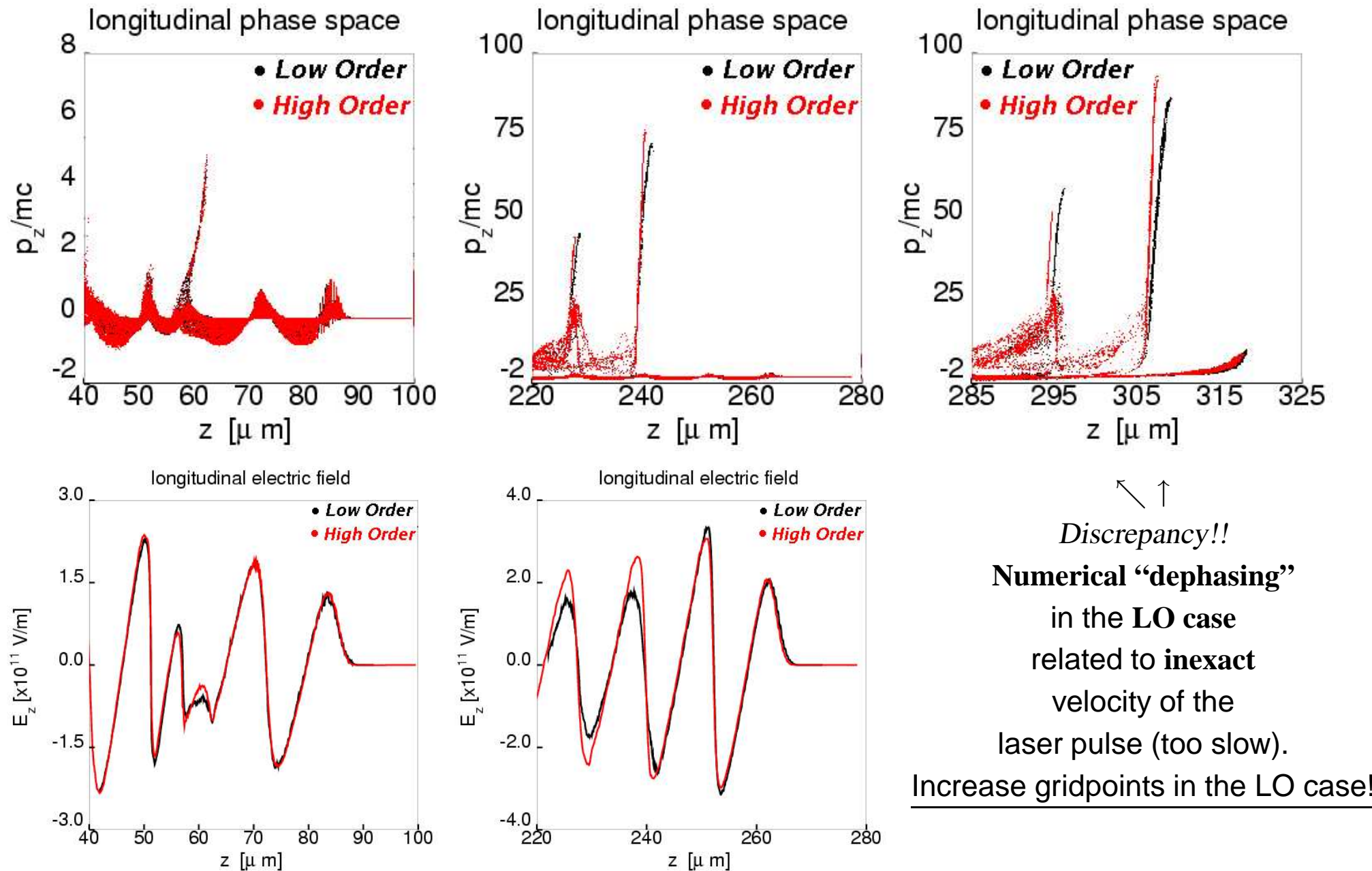
- domain: $(60 \times 80) \mu m^2$, grid: (750×200) points \Rightarrow **(10 × 2) points/λ**
- plasma sampled with: 20 electrons/cell
- derivatives: compact h.o. schemes (8^{th} order), time evolution: 4^{th} -order Runge-Kutta

- **ALaDyn Low Order** (14h on 4 CPUs)

- domain: $(50 \times 80) \mu m^2$, grid: (1200×320) points \Rightarrow **(20 × 3.2) points/λ**
- plasma sampled with: 20 electrons/cell
- derivatives: 2^{nd} -order accurate, time evolution: 2^{nd} -order accurate (leap-frog)

$$\frac{N_{HO}^{(grid)}}{N_{LO}^{(grid)}} = \frac{N_{HO}^{(particles)}}{N_{LO}^{(particles)}} = 0.4 \qquad \frac{\Delta t_{HO}}{\Delta t_{LO}} = 1.6$$

3. Benchmarks of the code: HO vs LO schemes



4. Application I: *ALaDyn* @ AO-FEL

AO-FEL= All-Optical Free Electron Laser ^a



- Generation of a **high-brightness, monochromatic** e^- -bunches from the interaction of an ultra-short & high-intensity **laser pulse** with a properly modulated gas-jet (nonlinear LWFA regime with longitudinal injection after density downramp)
- Interaction of the e^- -bunches with an **electromagnetic undulator** (*e.g.* CO₂ counterpropagating laser)

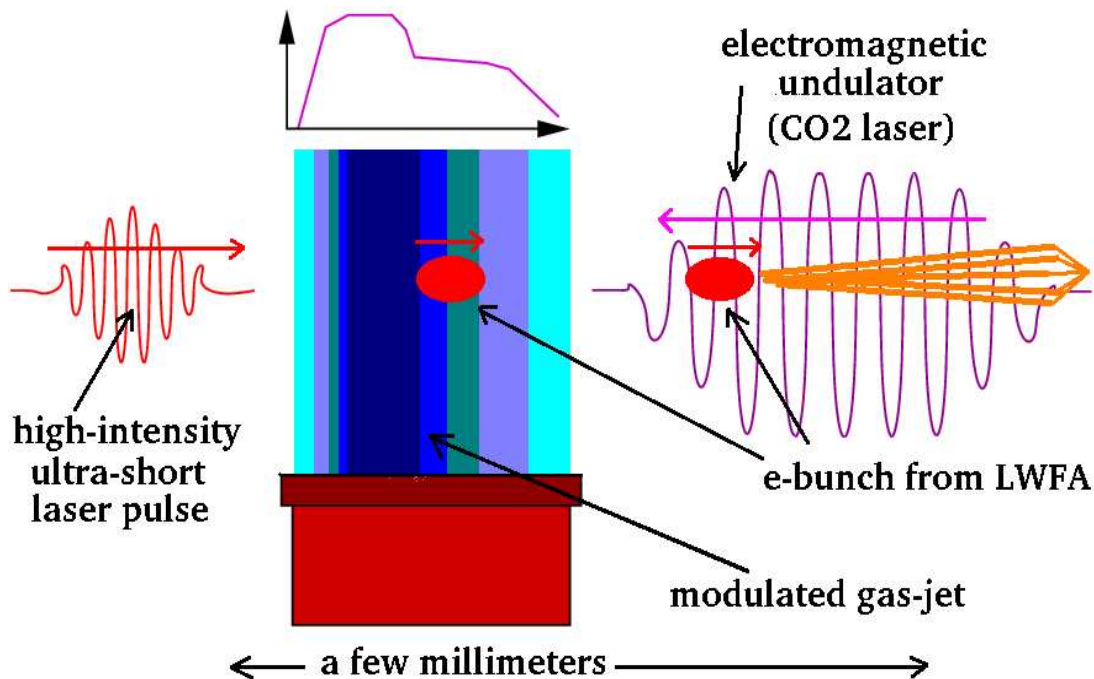
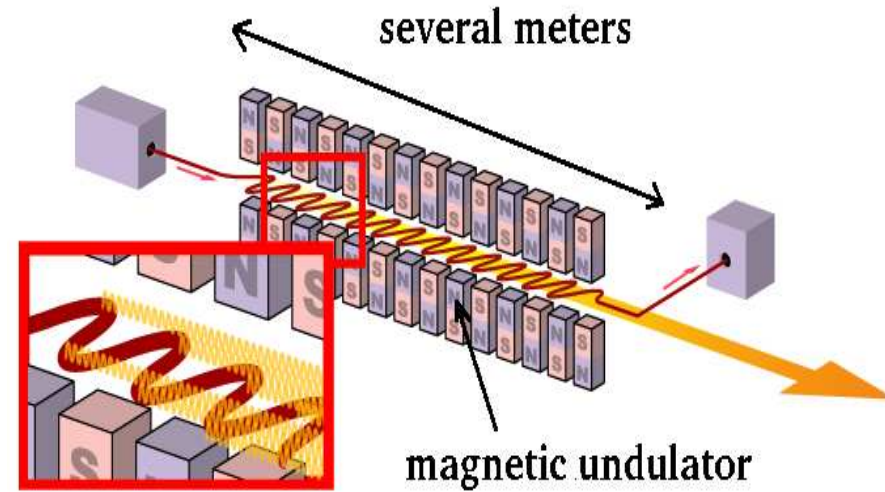
compact device for the production of coherent **X radiation** ($E_\nu=1$ [-10] keV, $\lambda=1$ [-0.1] nm)

» collaboration with V. Petrillo, L. Serafini, P. Tomassini @ INFN/Milano (work in progress!!) «

^aV. Petrillo, L. Serafini, P. Tomassini, PRSTAB **11**, 070703 (2008)

4. Application I: ALaDyn @ AO-FEL

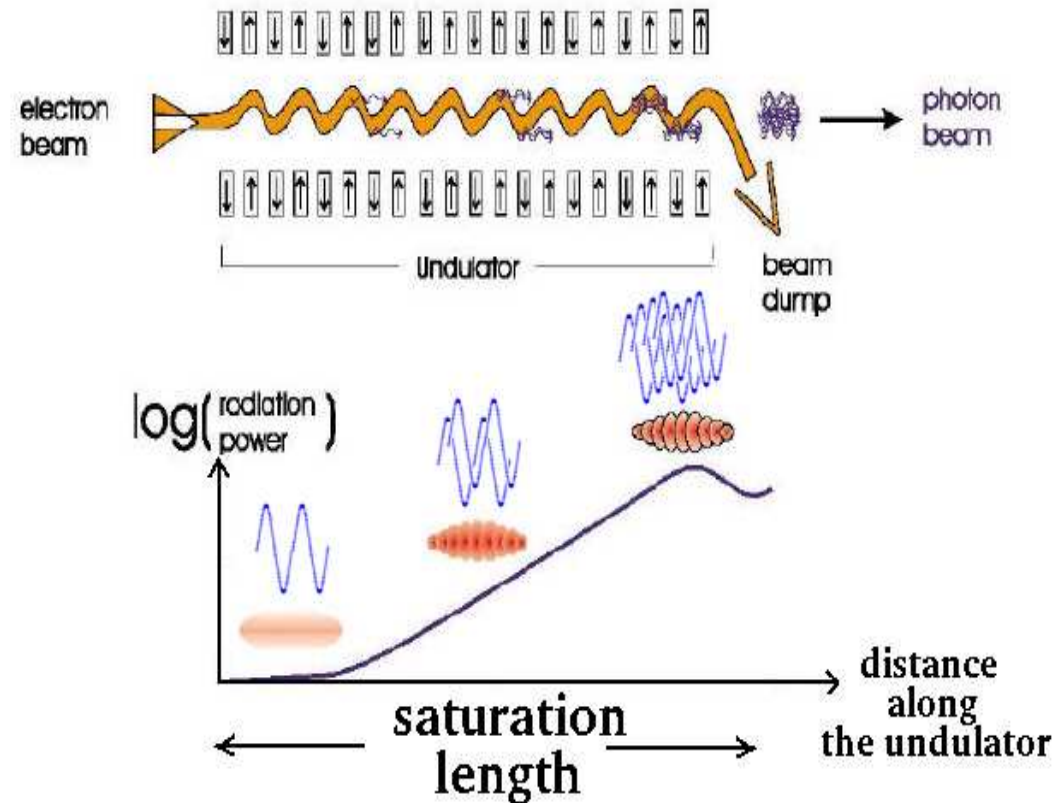
conventional FEL »»»»



«««« AO-FEL

4. Application I: ALaDyn @ AO-FEL

- Self-Amplified Stimulated-Emission (SASE) FEL



1. inside the undulator e^- emit EM radiation since they move in a curved path

2. e^- interact also with the generated EM radiation \Rightarrow this “feedback” causes the e^- -packing leading to the formation of microbunches

3. the coupling $e^- \leftrightarrow$ EM radiation is particularly efficient **when** there is “synchronization” between transverse oscillations of the e^- along the undulator and the oscillations of the co-moving EM field

4. the “resonant” radiation, which is **coherent**, reinforces itself **exponentially** along the undulator (positive feedback)

4. Application I: ALaDyn @ AO-FEL

1. Radiation emitted

$$\left\{ \begin{array}{l} \lambda_{rad} = \frac{\lambda_u}{2\gamma^2} \left(1 + \frac{K^2}{2} \right) \\ \lambda_{rad} = \frac{\lambda_u/2}{2\gamma^2} (1 + a_u^2) \end{array} \right. \quad \begin{array}{l} \text{static und.: } K \propto B_0 \lambda_u \ (\lambda_u \sim 10 \text{ mm}) \\ \text{EM und.: } \lambda_u/a_u = \text{waveleng./vect. poten. of the laser} \ (\lambda_u = 10 \text{ } \mu\text{m}) \end{array}$$

2. Pierce param.: conv. eff. e^- -beam power \rightarrow FEL rad. ($E_{FEL} = \rho E_{beam}$) \Rightarrow $\rho \propto \frac{I \lambda_u^{2/3}}{\gamma \sigma_x^{2/3}}$

3. Gain length: characteristic scale of the exponential amplification

$$L_{gain} = (1 + \eta) \frac{\lambda_u}{4\pi\sqrt{3}\rho} \quad (\eta \text{ is a correction factor: depends on } \epsilon_n, \delta\gamma/\gamma, \sigma_x, \dots)$$

4. requirements for the FEL growth: $\frac{\delta\gamma}{\gamma} < \sqrt{3}\rho \quad \epsilon_{n,x} < \sqrt{\frac{\lambda_{rad}}{4\pi L_{gain}}} \gamma \sigma_x$

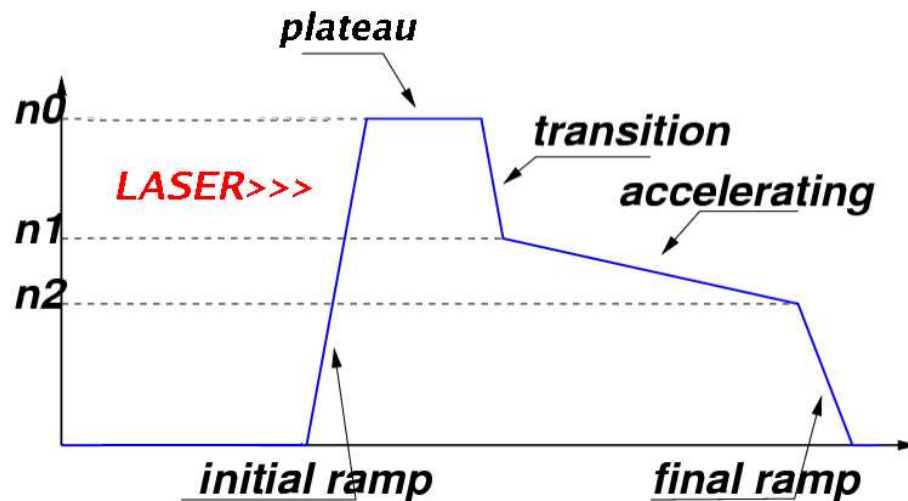
N.B. the relevant $\delta\gamma/\gamma$ is taken over a **bunch slice** of length $L_c = \lambda_{rad}/(4\pi\sqrt{3}\rho)$ [**cooperation length**]. The bunch **do not need** to be characterized by **overall** low $\delta\gamma/\gamma$ and ϵ_n : it should **contain slices** with low $\delta\gamma/\gamma$ and ϵ_n instead.

$$\lambda_{rad}, L_{gain} \text{ with EMU} \ll \lambda_{rad}, L_{gain} \text{ with SU for the same } \gamma, \text{ but higher } I \text{ is needed}$$

4. Application I: ALaDyn @ AO-FEL

• **ALaDyn** \Rightarrow generation of a **high current** e^- bunch containing slices with **low emittance** and **low momentum spread** from laser-plasma interaction

\Rightarrow we choose the nonlinear LWFA regime with **longitudinal wave breaking at density downramp** [S. Bulanov *et al.*, PRE **58/5**, R5257 (1998)]: better beam quality than the **bubble regime** (but with lower charge)



1. the local wave number k_p of a plasma wave satisfies

$$\partial_t k_p = -\partial_z \omega_p$$

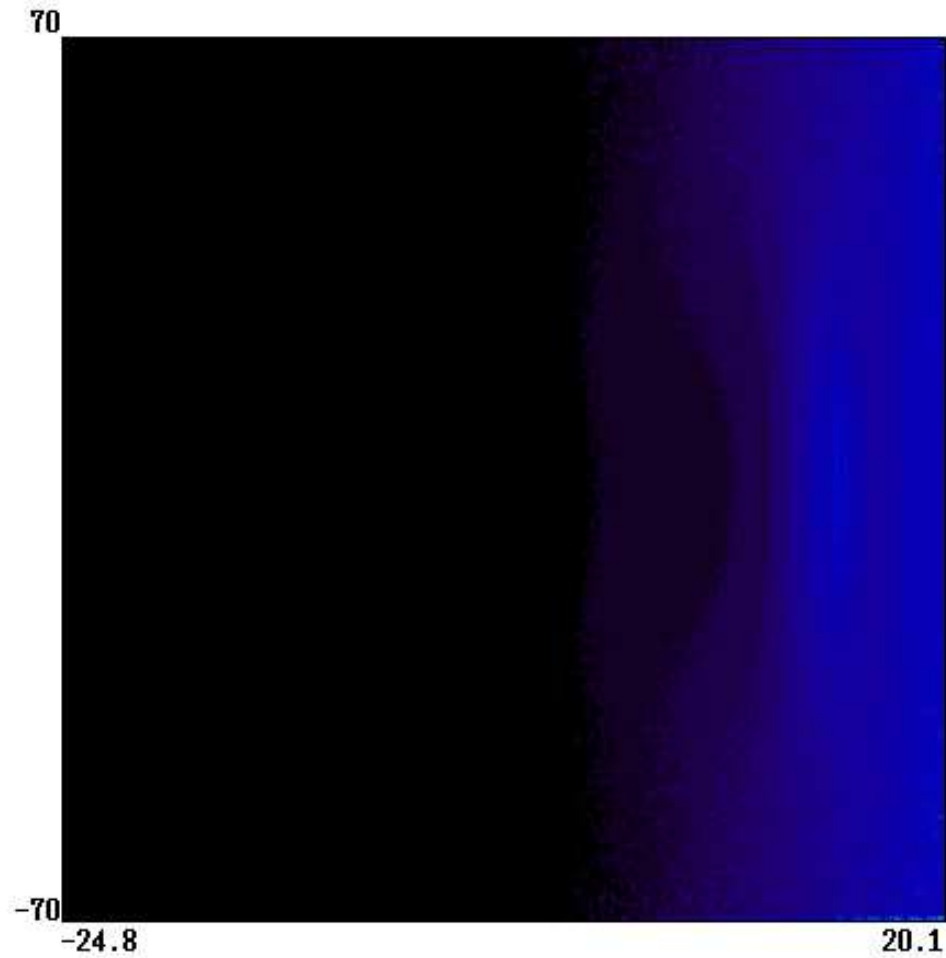
2. if the wave moves from a high-density to a low-density zone then k_p increases in time \Rightarrow the phase velocity of the p. w. $v_{phase} = \omega_p/k_p$ decreases

3. if the quiver velocity of the electrons in the wave is larger than v_{phase} , the wave **breaks**

$$n_{inj} \propto \bar{n}/\ell_{trans}, \text{ where } \bar{n} = (n_0 + n_1)/2$$

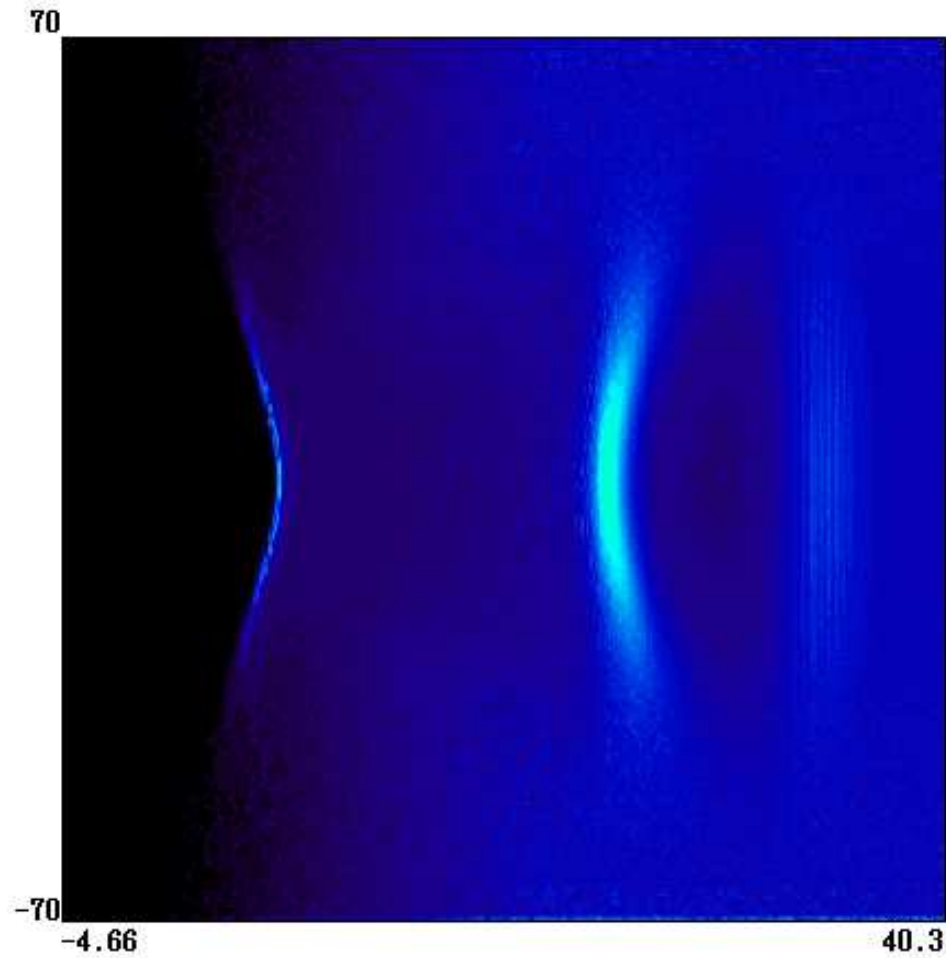
4. Application I: ALaDyn @ AO-FEL

- Electron density in the plane (z, x) , $t = 67$ fs



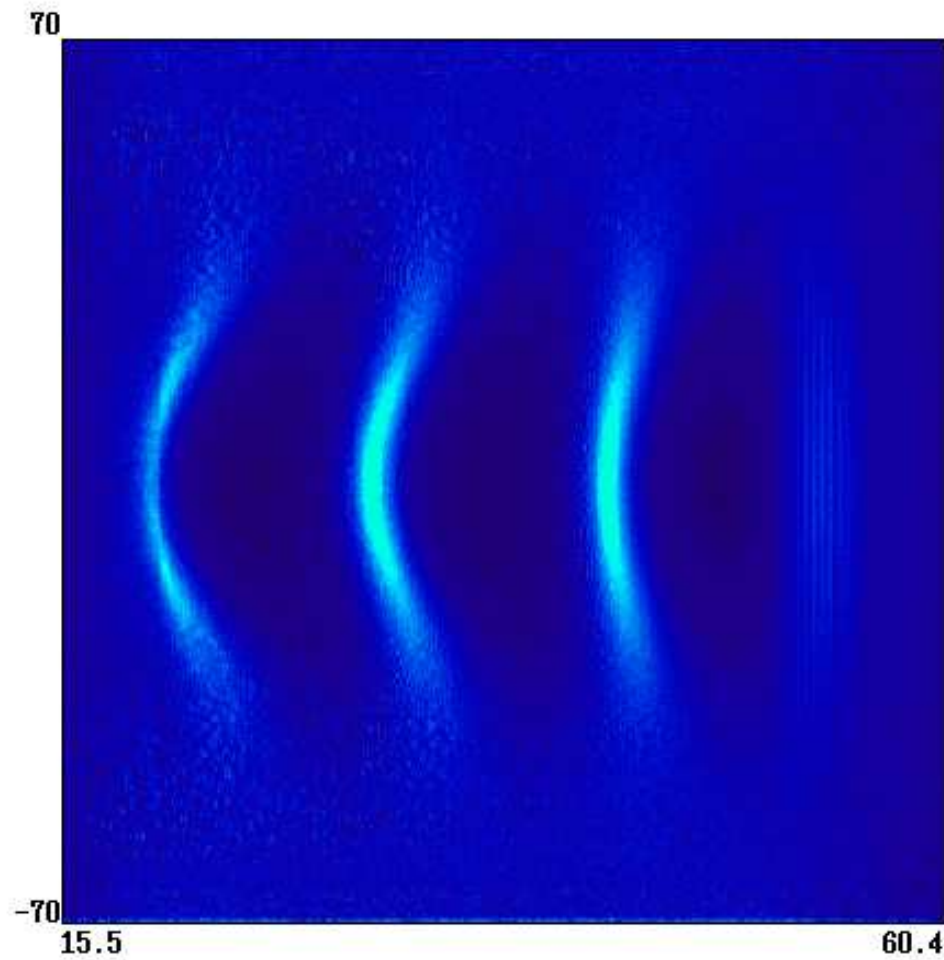
4. Application I: ALaDyn @ AO-FEL

- Electron density in the plane (z, x) , $t = 133$ fs



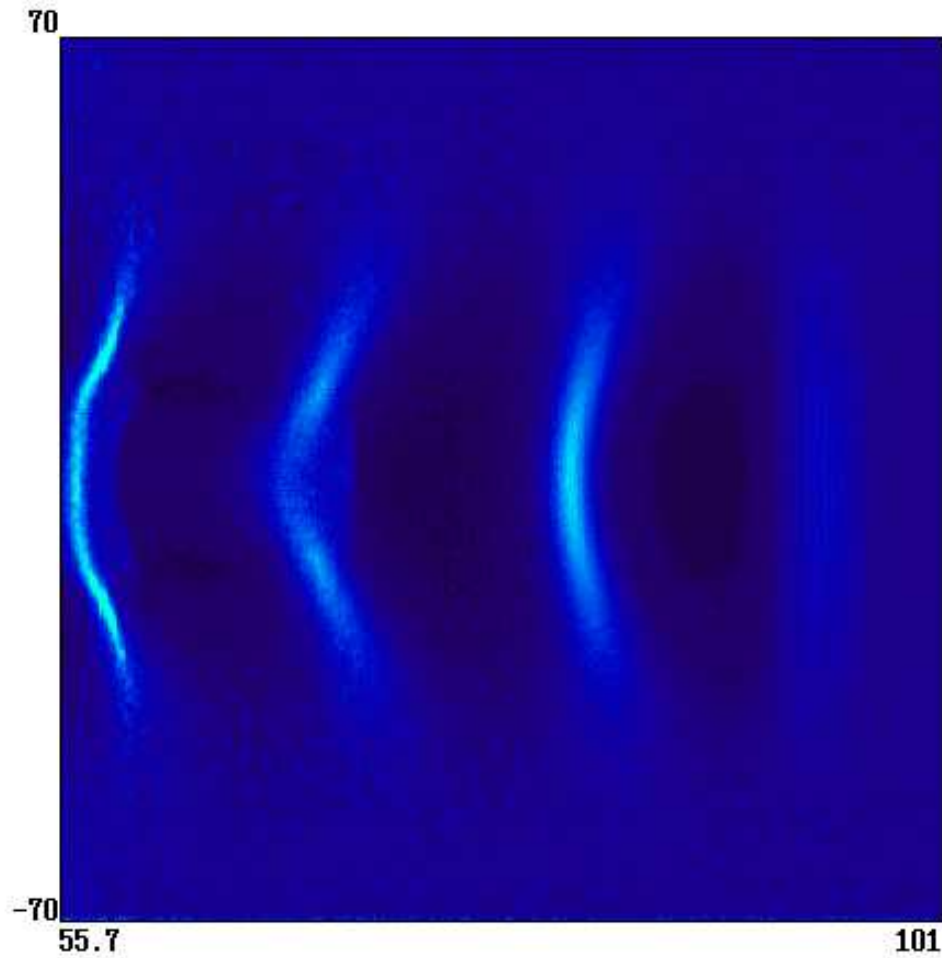
4. Application I: ALaDyn @ AO-FEL

- Electron density in the plane (z, x) , $t = 201$ fs



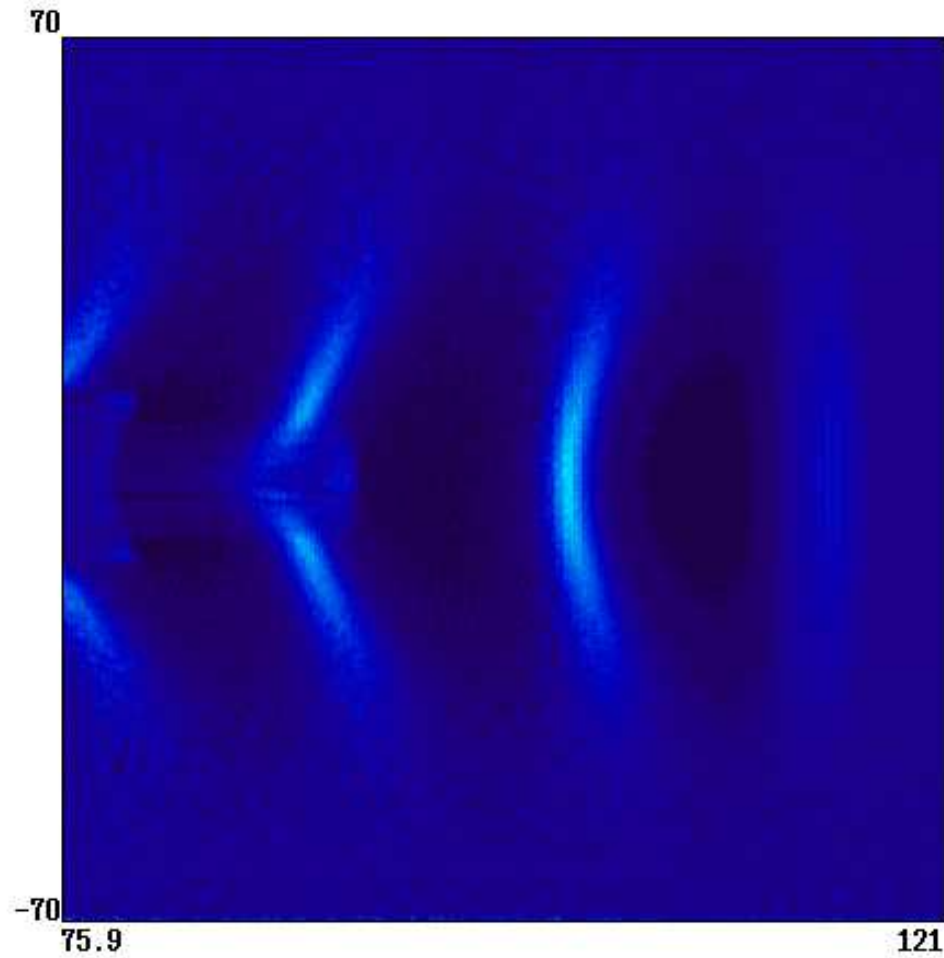
4. Application I: ALaDyn @ AO-FEL

- Electron density in the plane (z, x) , $t = 335$ fs



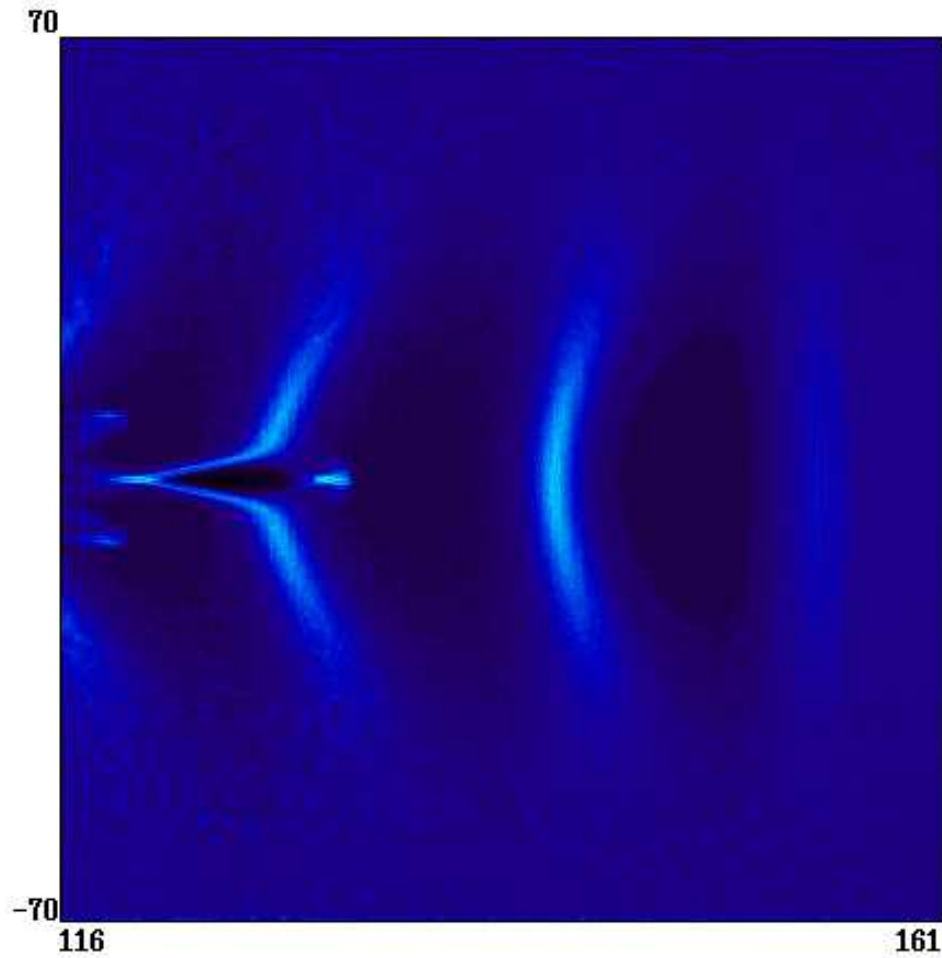
4. Application I: ALaDyn @ AO-FEL

- Electron density in the plane (z, x) , $t = 402$ fs



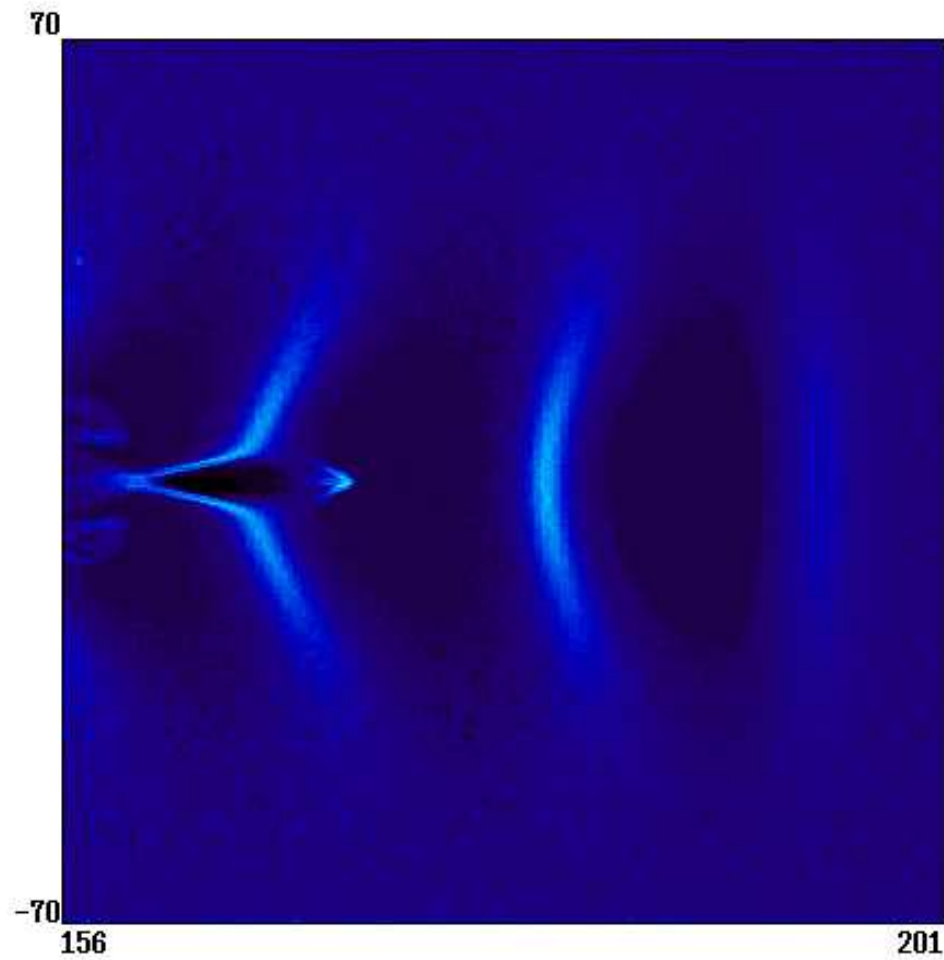
4. Application I: ALaDyn @ AO-FEL

- Electron density in the plane (z, x) , $t = 536$ fs



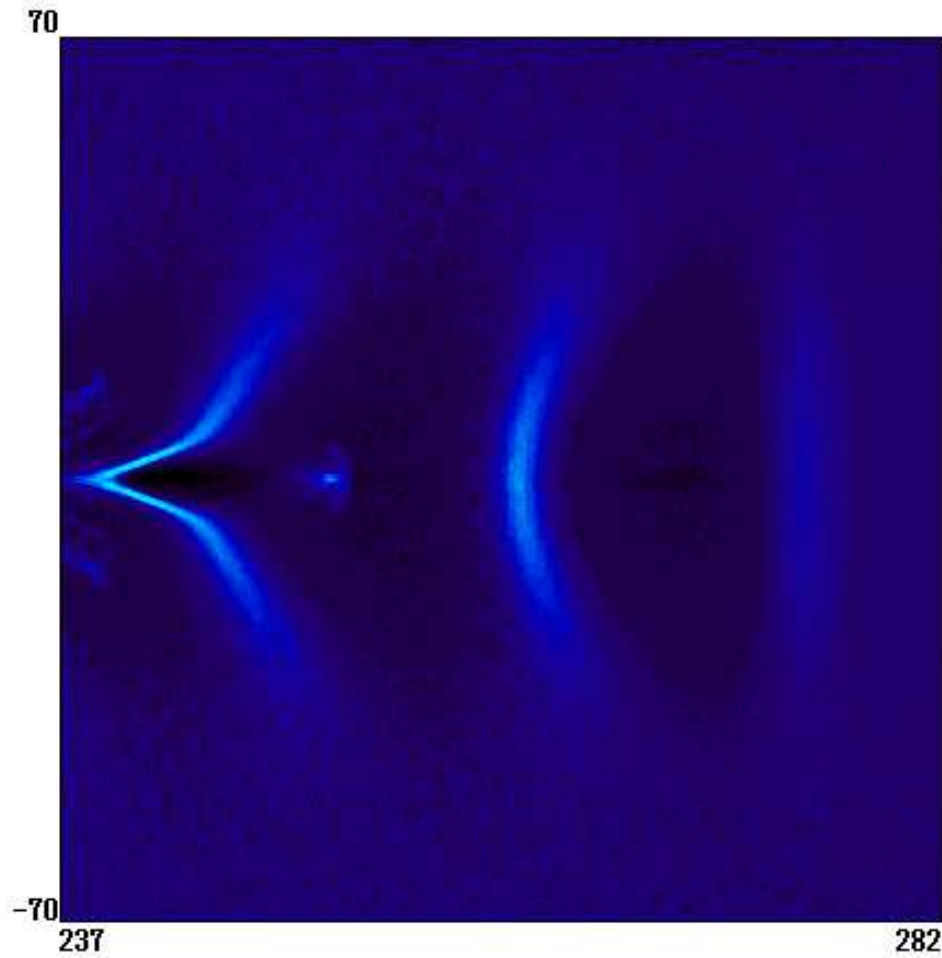
4. Application I: ALaDyn @ AO-FEL

- Electron density in the plane (z, x) , $t = 669$ fs



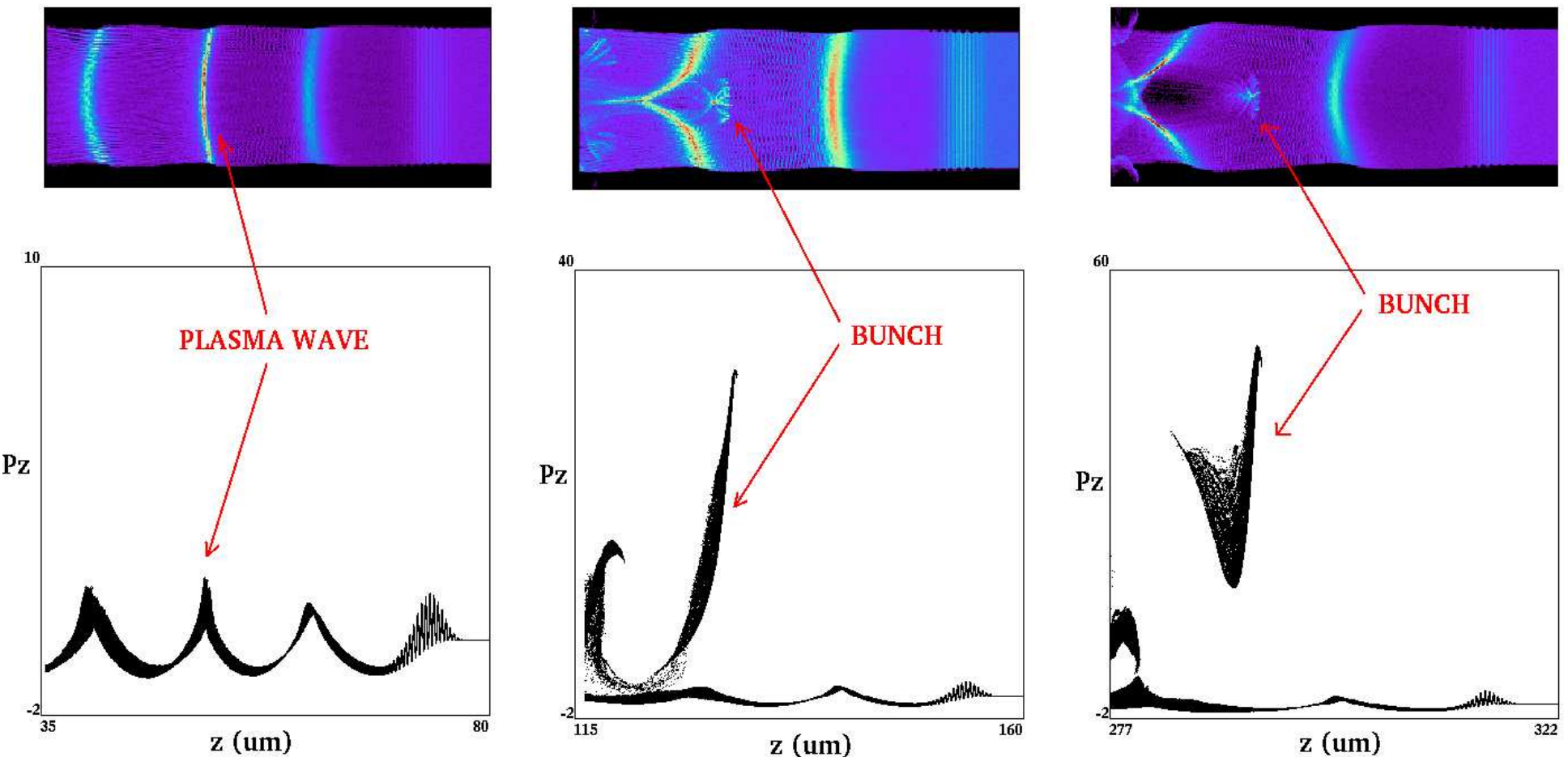
4. Application I: ALaDyn @ AO-FEL

- Electron density in the plane (z, x) , $t = 936$ fs



4. Application I: ALaDyn @ AO-FEL

- Simulation (2D) of the wave breaking + injection: electron density (top) & longitudinal phase space (bottom)



4. Application I: ALaDyn @ AO-FEL

- Computational “challenges”:

1. determine the density profile which gives a **“satisfying” bunch**: more than 50 **2D simulations** for parameter scan & convergence check (changing num. parameters)
 - domain: $(45 \times 120) \mu\text{m}^2$
 - resolution: (up to) 22 points/ μm (long.)/ 12 points/ μm (transv.), 50 particles/cell

\Rightarrow we work in the case $w_{laser} > \lambda_p$, $c\tau_{FWHM} < \lambda_p$ and we consider short interaction lengths (less than $100 \mu\text{m}$): the dynamics of the wave breaking is “almost” 1D (longitudinal) and we don’t expect big differences between 2D and 3D simulations
2. study (with **sub- μm resolution**) the properties of the small (**a few microns**) electron bunch in a fully 3D simulation
 - domain: $(45 \times 120 \times 120) \mu\text{m}^3$
 - resolution: 15 points/ μm (long.)/ 12 points/ μm (transv.), 4-5 particles/cell

LF2/NO Stretched grid/NO hierarch. part. samp.	ALaDyn
$1300 \times 1440^2 > 10^9$ part.	$675 \times 200^2 \quad 140 \cdot 10^6$ part.

factor ~ 100 gain with ALaDyn

4. Application I: ALaDyn @ AO-FEL

- **Laser parameters:**

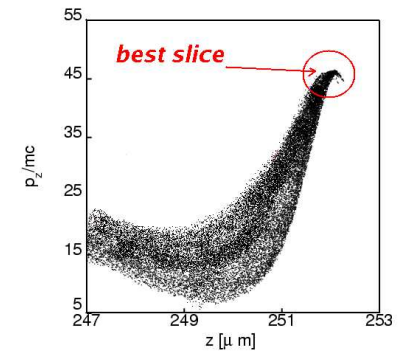
λ_0 [μm]	I [W/cm^2]	τ_{FWHM} [fs]	waist [μm]
0.8	8.5×10^{18}	17	23

- **Plasma profile:**

n_0 [$\times 10^{19} \text{cm}^{-3}$]	ℓ_{trans} [μm]	n_1 [$\times 10^{19} \text{cm}^{-3}$]	L_{acc} [μm]	n_2 [$\times 10^{19} \text{cm}^{-3}$]
1.0	10	0.75	330	0.4

- **Bunch from 2D simulation:**

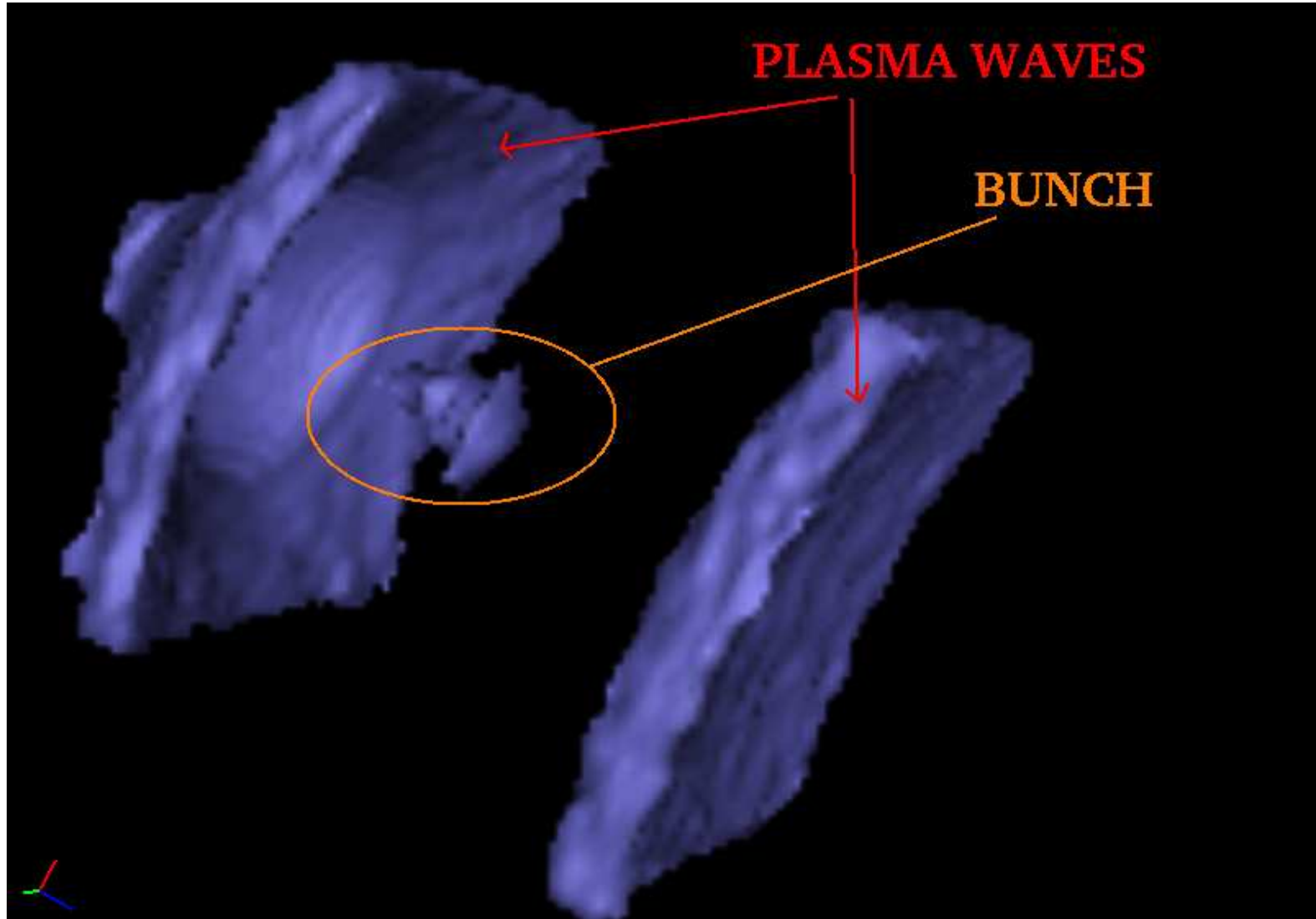
γ	σ_z [μm]	Q [pC]	$(\delta\gamma/\gamma)^s$ [%]	ϵ_n^s [mm mrad]	I^s [kA]
50	1.5	200	0.3	0.1	5-7



\Rightarrow current too low ?

4. Application I: ALaDyn @ AO-FEL

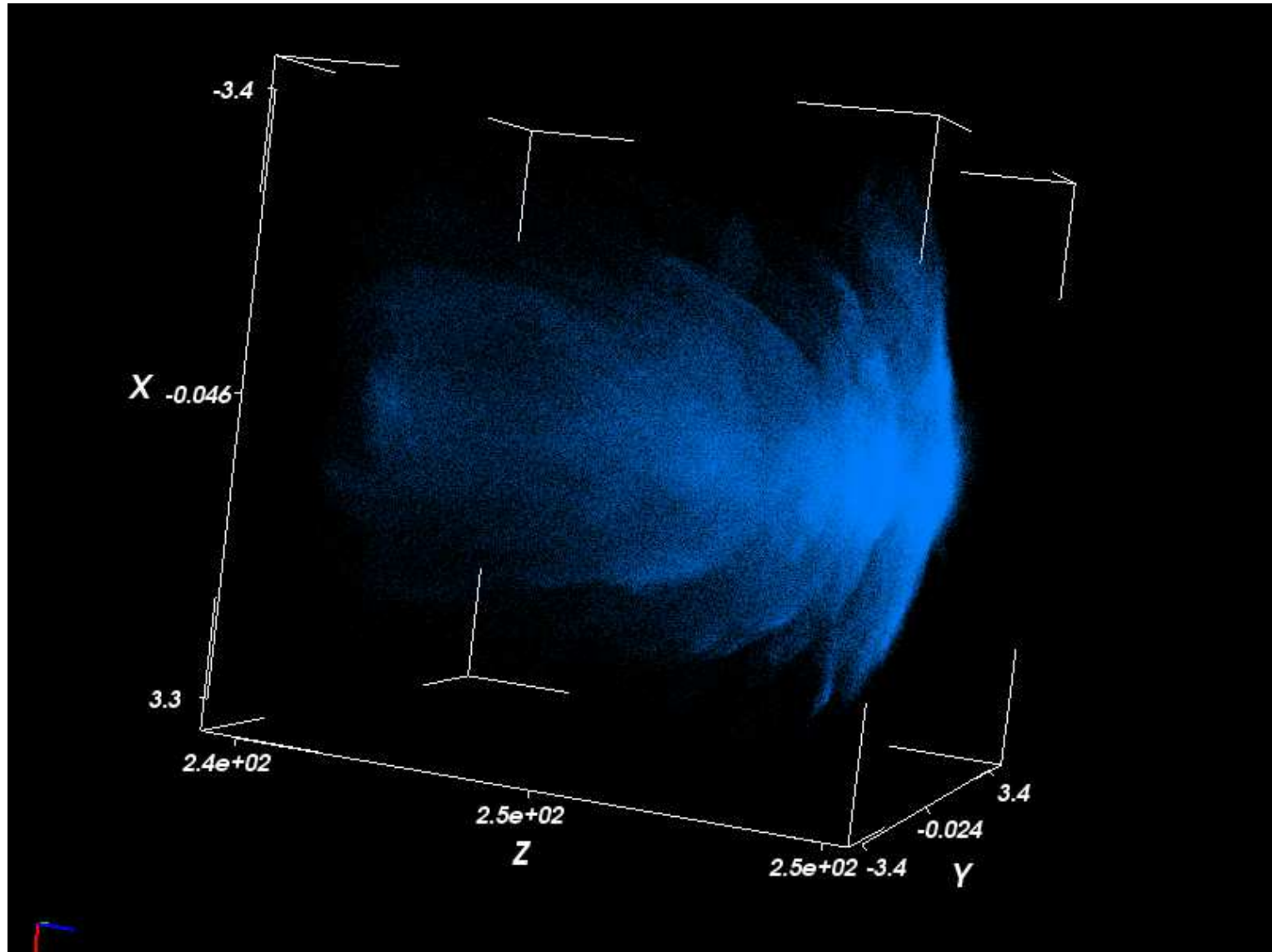
- Snapshot* of the 3D simulation done @ CINECA (Italy) on 72CPUs (electron density)



* rendering with VisIVO

4. Application I: ALaDyn @ AO-FEL

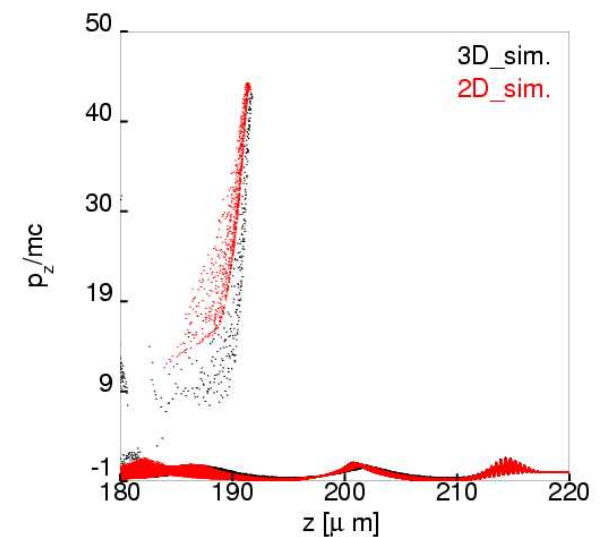
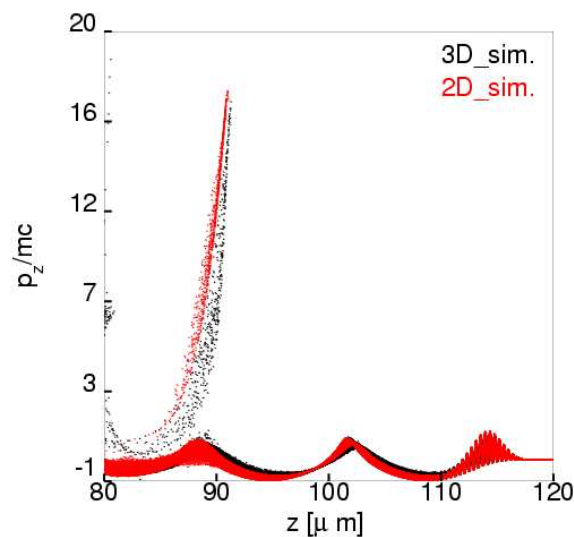
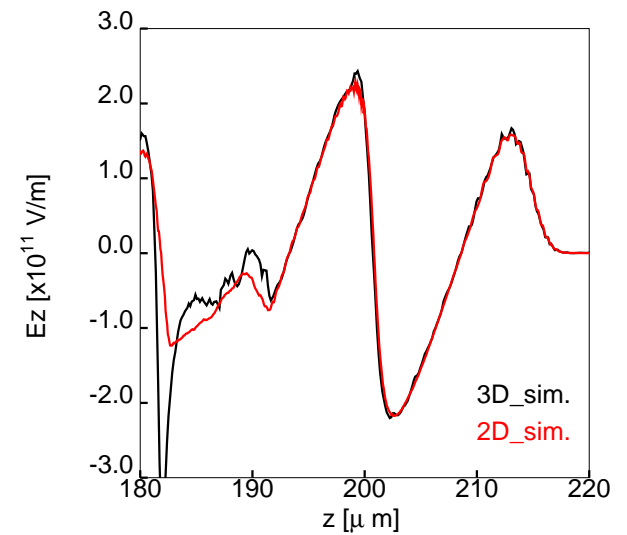
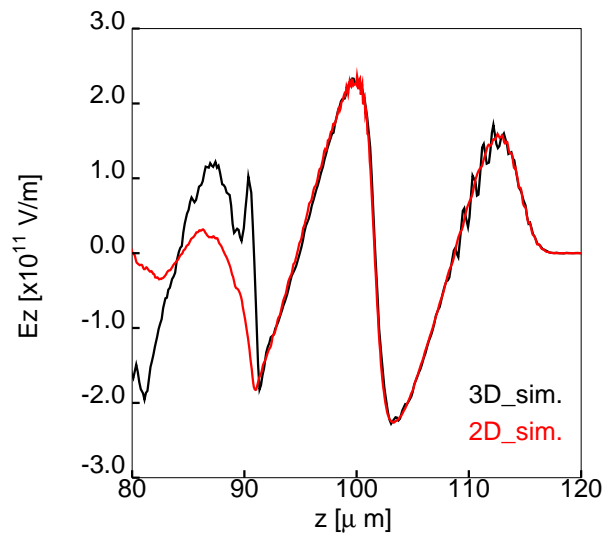
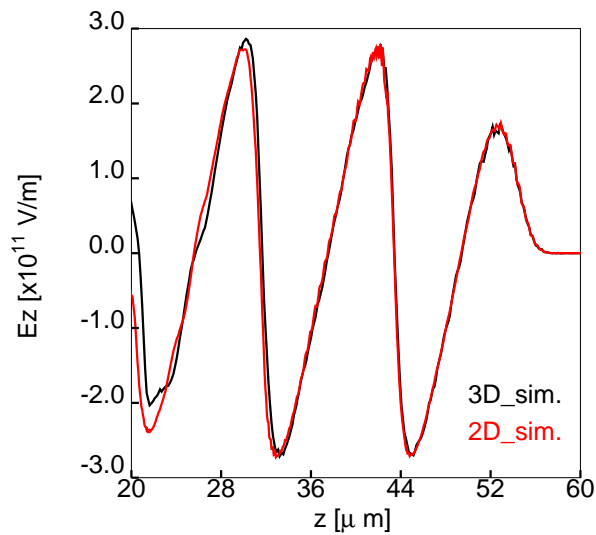
- Close-up of the e^- bunch* in the 3D simulation done @ CINECA (Italy) on 72CPUs



* rendering with VisIVO

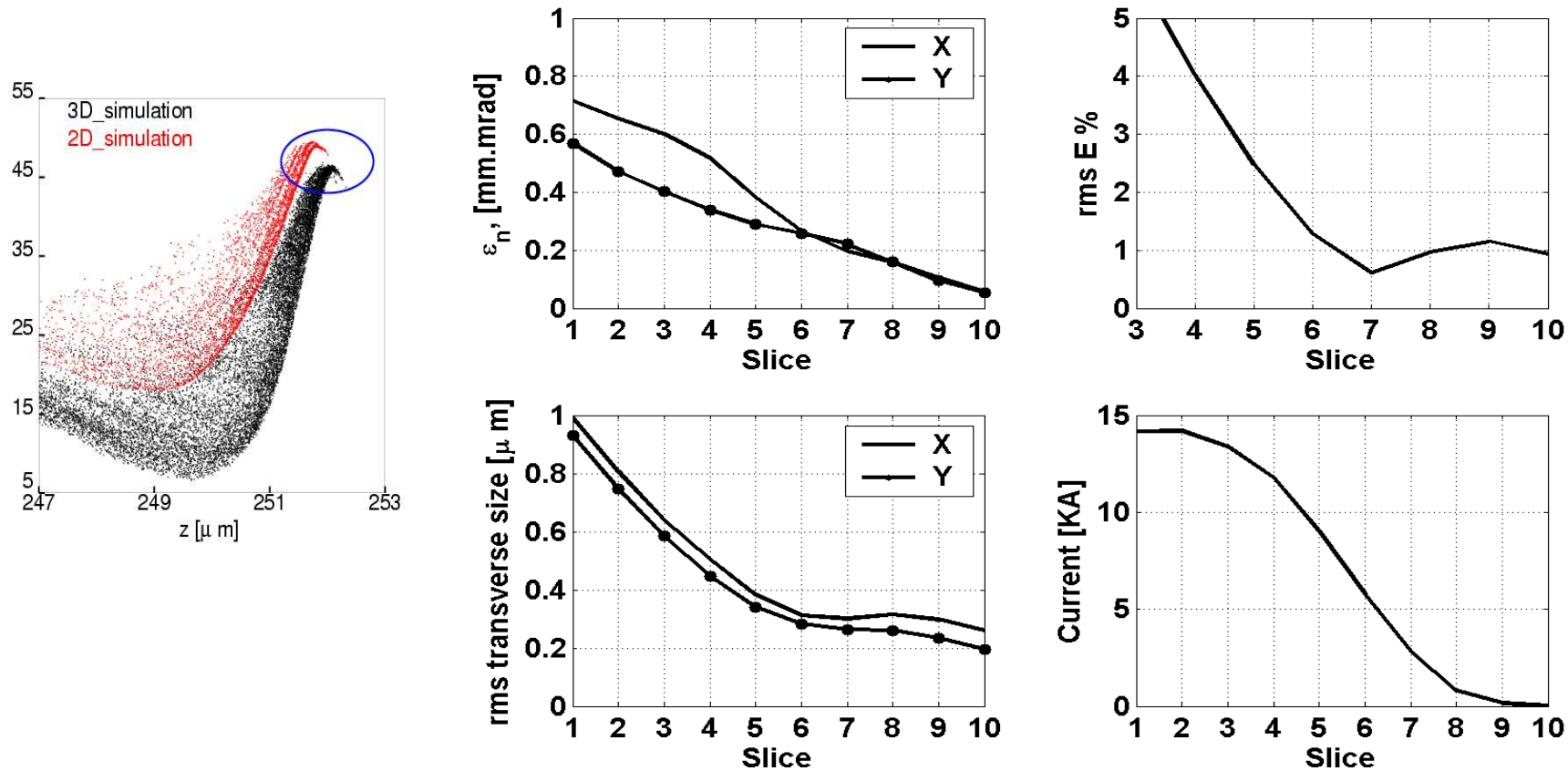
4. Application I: ALaDyn @ AO-FEL

- Comparison 2D/3D (longitudinal field/phase space)



4. Application I: ALaDyn @ AO-FEL

- Slice analysis of the 3D accelerated bunch (*not too different from 2D*)

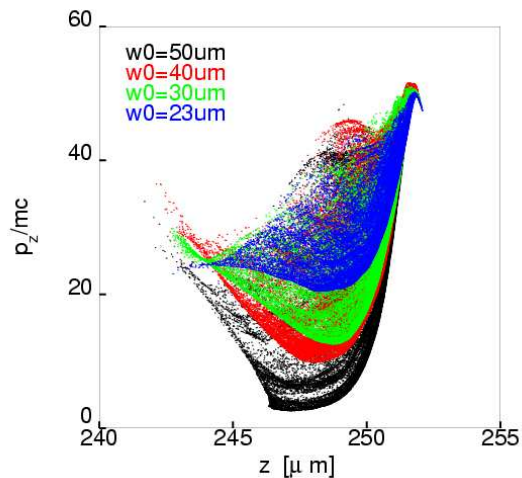


γ	σ_z [μm]	Q [pC]	$(\delta\gamma/\gamma)^s$ [%]	ϵ_n^s [mm mrad]	$\sigma_{x,y}^s$ [μm]	I^s [kA]
45	1.7	160	0.55	0.2	0.3	4-5

\Rightarrow current too low to drive the FEL instability ($I^s > 15 - 20$ kA is required)!

4. Application I: ALaDyn @ AO-FEL

- 1 the most practical way to increase the current is to **increase** w_0 to **collect more charge** during the wave breaking $\Rightarrow Q \propto w_0^2$
- 2 σ_z is determined only by ℓ_{trans} (doesn't depend on w_0) $\Rightarrow I \propto w_0^2$
- 3 the dynamics is $\sim 1D$ (small transverse effects): the r.m.s. parameters of the best slices (the ones in the front part) are not affected by the increase in w_0



w_0 [μm]	σ_z [μm]	Q_{bunch} [pC]	I^s [kA]	I^s/w_0^2
23	1.50	200	6.8	0.013
30	1.55	370	9.8	0.011
40	1.46	610	21	0.013
50	1.56	1000	31	0.012

\Rightarrow in all the (2D) simulations changing w_0 we obtained $(\delta\gamma/\gamma)^s \sim 0.3\%$, $\epsilon_n^s \sim 0.1$ mm mrad

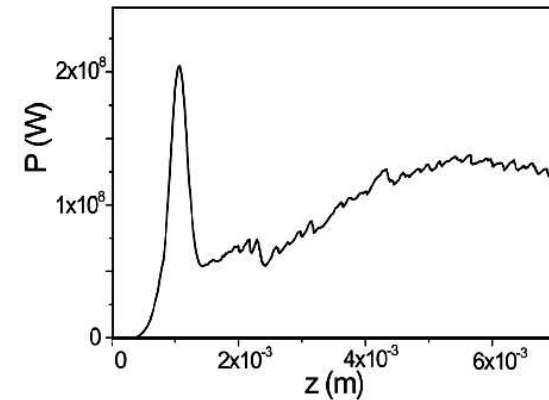
we are waiting for FEL simulations: ALaDyn beam + CO₂ EM undulator ($\lambda_u = 10.6 \mu\text{m}$, $a_u = 0.8$)

4. Application I: ALaDyn @ AO-FEL

- FEL simulations (by V. Petrillo): beam (not the best one) + CO₂ EM undulator ($\lambda_u = 10.6 \mu\text{m}$, $a_u = 0.8$) simulated with GENESIS 1.3

$$\lambda_{rad} = 1.3 \text{ nm}$$

	First peak	Saturation
P_{max} [MW]	200 (0.3 fs FWHM)	150
E [μJ]	0.05	0.5
L_{sat} [mm]	1	4



Laser requirements for the undulator: 250 GW for 5 mm, $w_u = 30 \mu\text{m}$, $E_u = 4 \text{ J}$

- the possibility to produce radiation with $\lambda_{rad}=1 \text{ \AA}$ considering a Ti:Sa undulator ($\lambda_u = 0.8 \mu\text{m}$) is currently under investigation (in this case a high power laser is required for the undulator)

5. Application II: *ALaDyn* @ PLASMONX

5. Application II: ALaDyn @ PLASMON-X

PLASMONX= PLASma acceleration & MONochromatic X-ray production (2009-.....)

combining the high brightness LINAC accelerator of the SPARC@LNF project with the ultrashort (~ 20 fs), high power (300 TW) FLAME laser

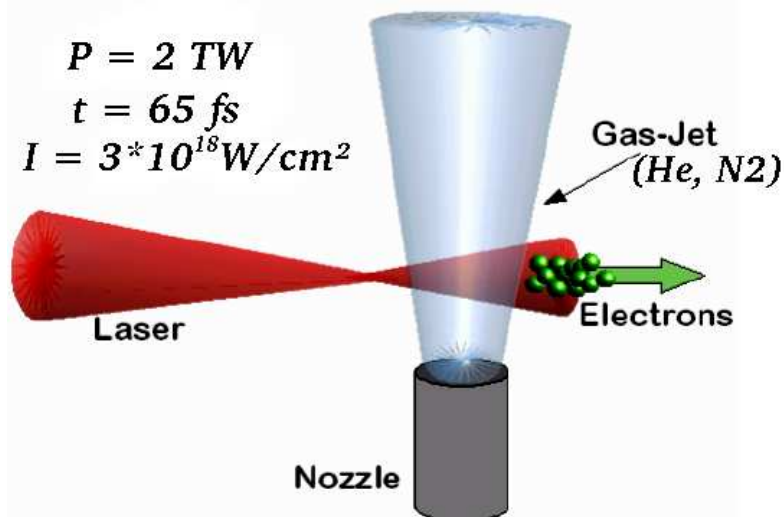
- Scheduled activity:
 - LWFA with both self and externally injected e -beams;
 - Linear and nonlinear Thomson Scattering for X/ γ -ray source: backscattering of the laser pulse on both LINAC and LWFA e -beams;
 - Intense laser-matter interaction, proton acceleration.

5. Application II: ALaDyn @ PLASMON-X

“PILOT” self-injection experiment (at reduced power)

*L.A.Gizzi^(1,2), C.Benedetti⁽³⁾, S.Betti⁽¹⁾, C.A.Cecchetti^(1,2), A.Gamucci^(1,2), A.Giulietti^(1,2),
D.Giulietti^(1,2), P.Koester^(1,2), L.Labate^(1,2), F.Michienzi^(1,2), N.Pathak^(1,2), A.Sgattoni⁽³⁾,
G.Turchetti⁽³⁾, F.Vittori^(1,2)*

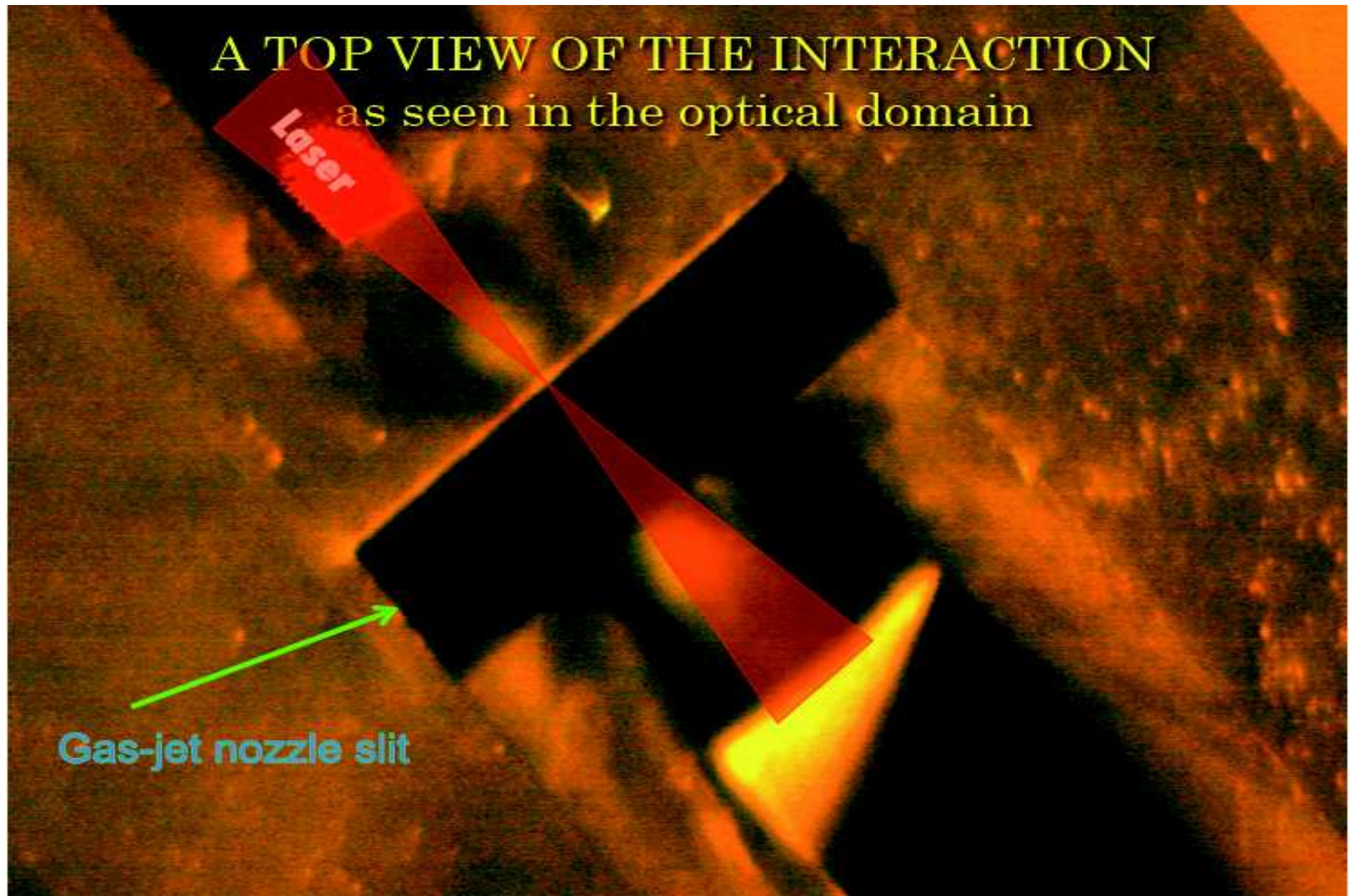
(1) *ILIL-CNR, Pisa (Italy)*, (2) *INFN, Pisa (Italy)*, (3) *University of Bologna & INFN/Bologna (Italy)*



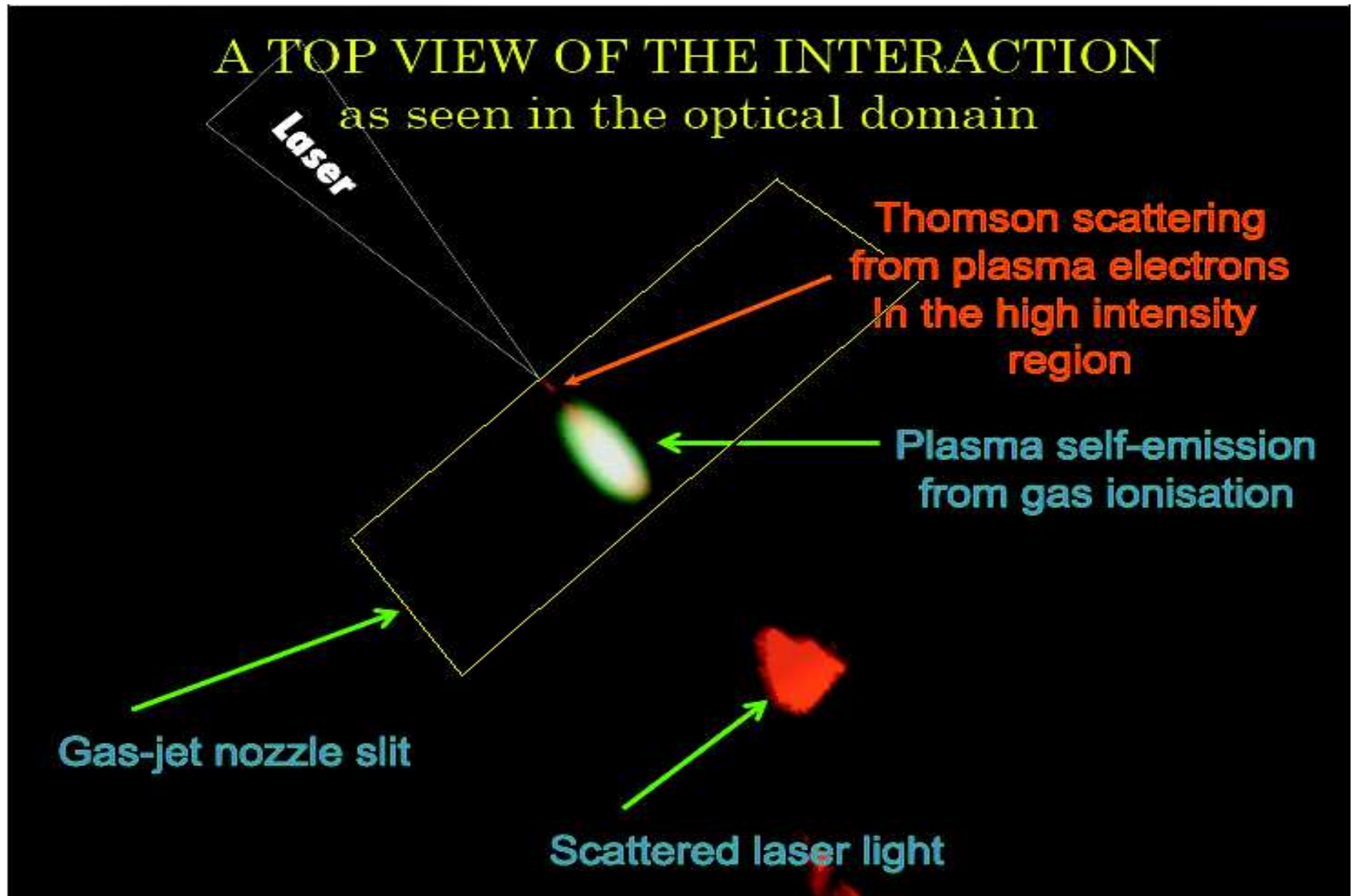
Main tasks:

- 1 establish table-top acceleration conditions using low power (2 TW) fs laser systems;
- 2 expertise build-up for risk-mitigation in large scale (FLAME, 300 TW) approach to high quality laser-driven acceleration.

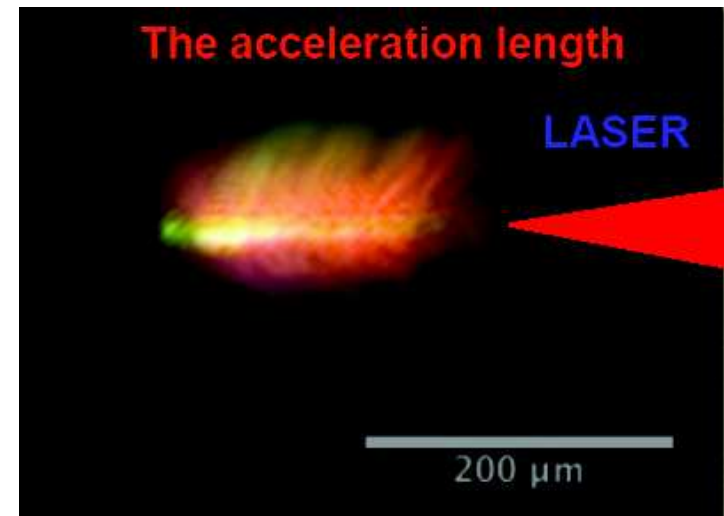
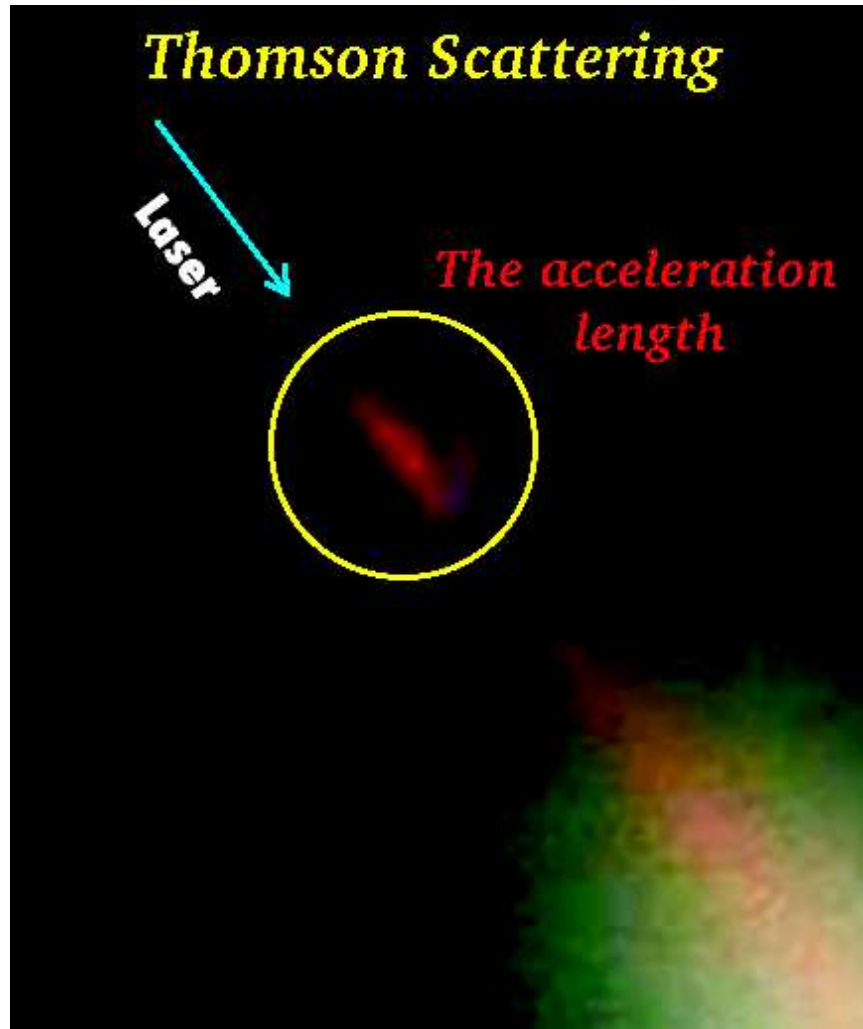
5. Application II: ALaDyn @ PLASMON-X



5. Application II: ALaDyn @ PLASMON-X



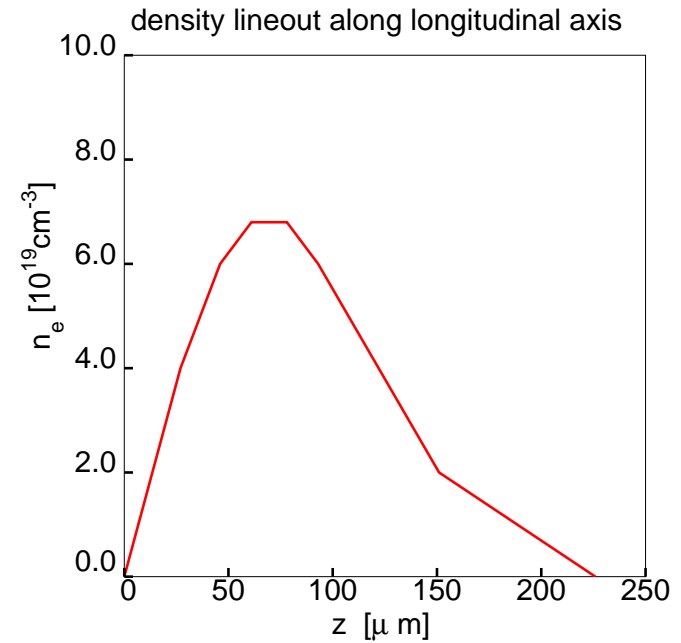
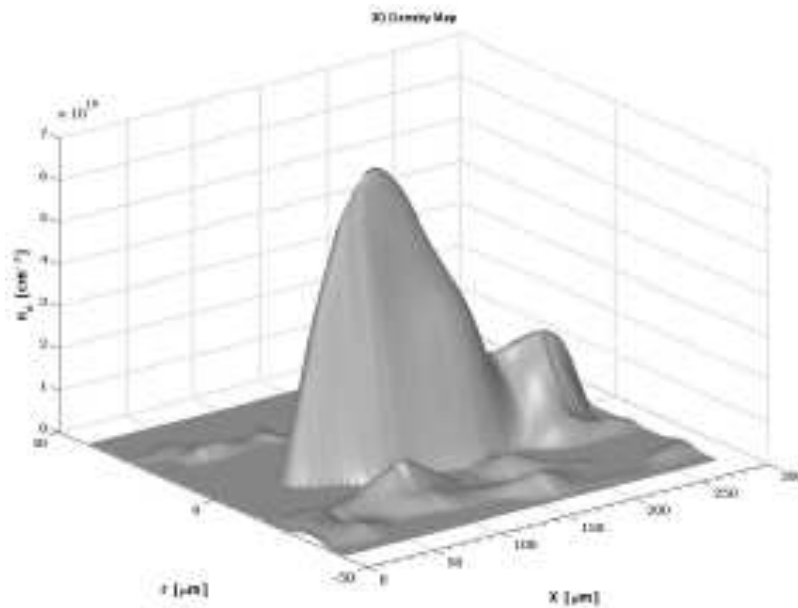
5. Application II: ALaDyn @ PLASMON-X



Thomson scattering clearly shows the region of propagation of the laser pulse, with evidence of self-guiding over a length approximately three times the depth of focus ($\sim 50 \mu\text{m}$).

5. Application II: ALaDyn @ PLASMON-X

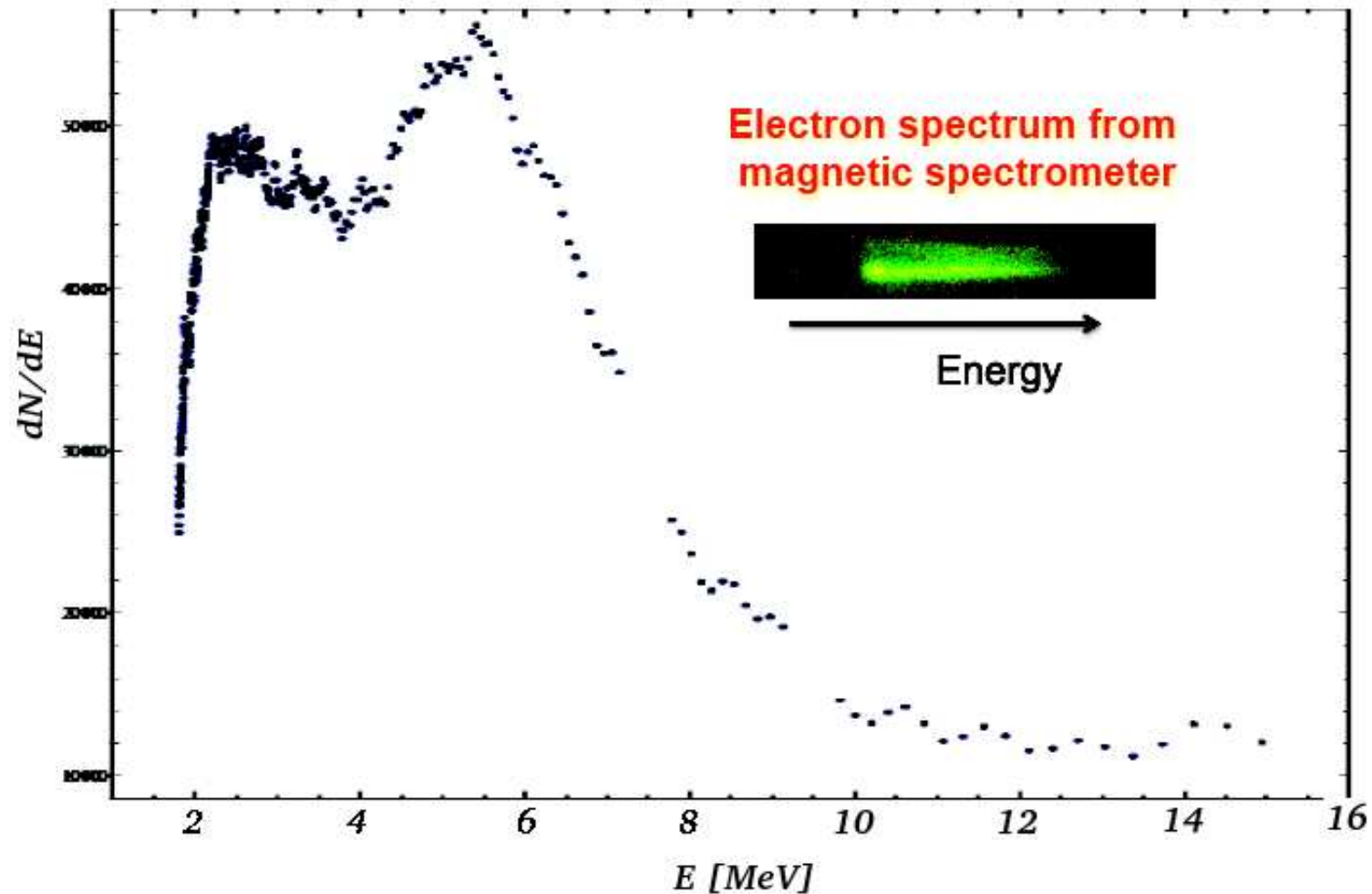
- Electron plasma density (from interferometry)



\Rightarrow peak electron density $\sim 7 \times 10^{19} \text{ cm}^{-3}$

\Rightarrow channel length $\sim 200 \div 250 \mu\text{m}$

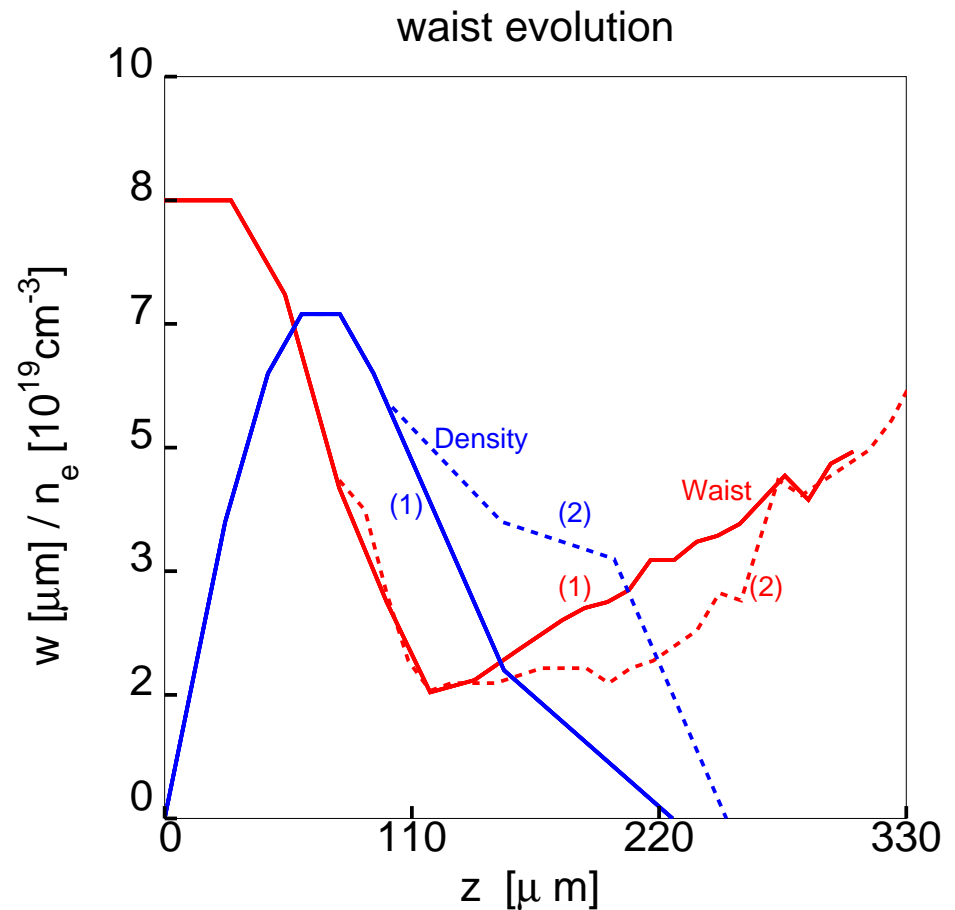
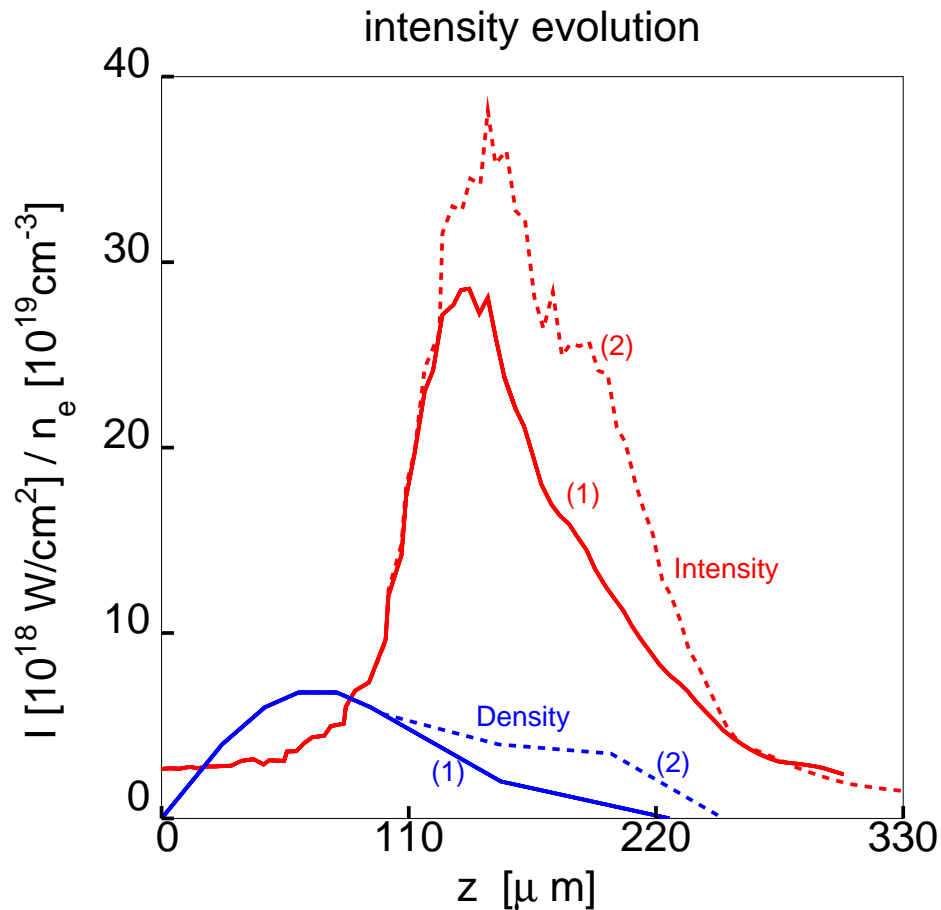
5. Application II: ALaDyn @ PLASMON-X



electron energy peak	e -beam divergence	e -beam reprod.	bunch charge
5-6 MeV	$\sim 10^\circ$	good	$\gtrsim 0.1 \text{ nC}$

5. Application II: ALaDyn @ PLASMON-X

Laser evolution in the plasma

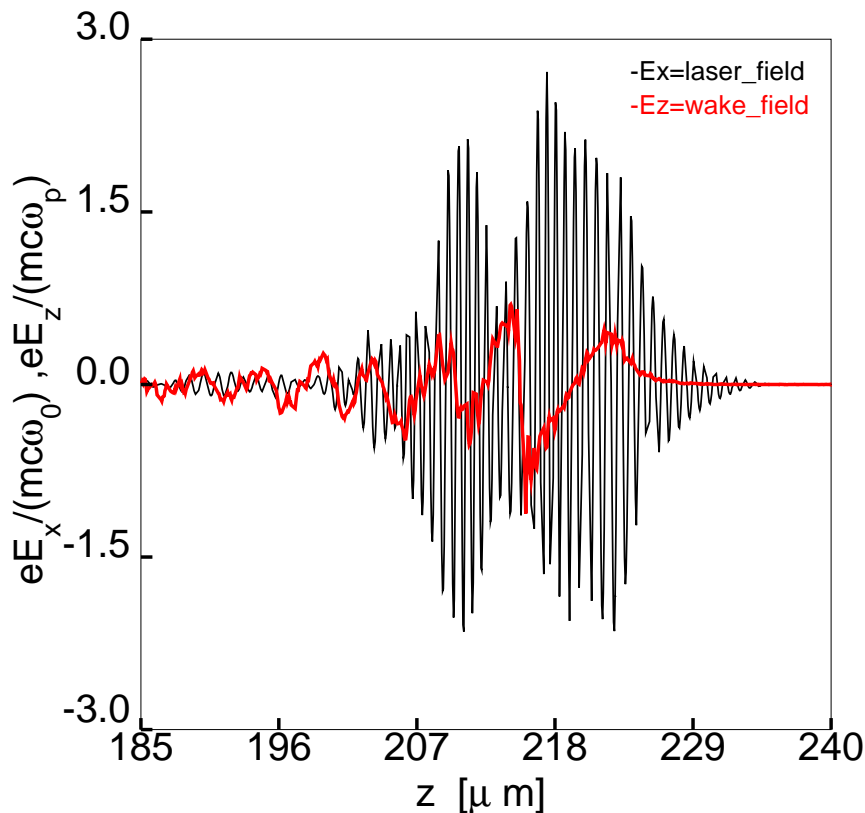
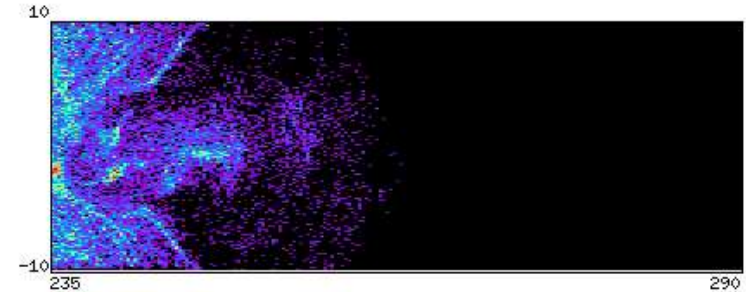
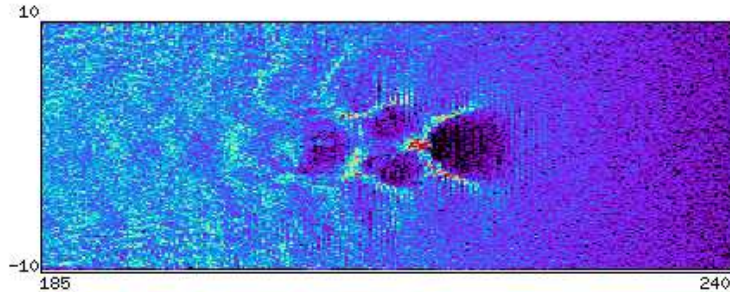


⇒ We have considered two different density profiles in order to take into account shot-to-shot variability

⇒ Strong self-focusing occurs leading to a ~ 10 -fold increase of the local intensity

5. Application II: ALaDyn @ PLASMON-X

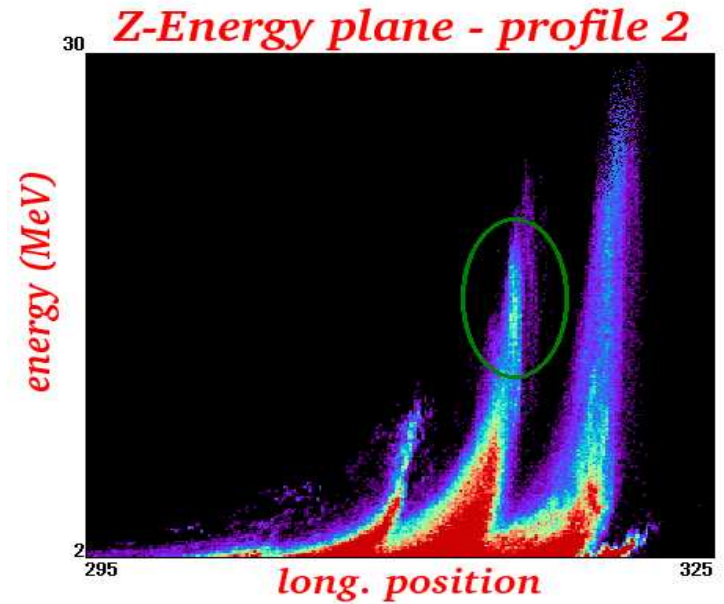
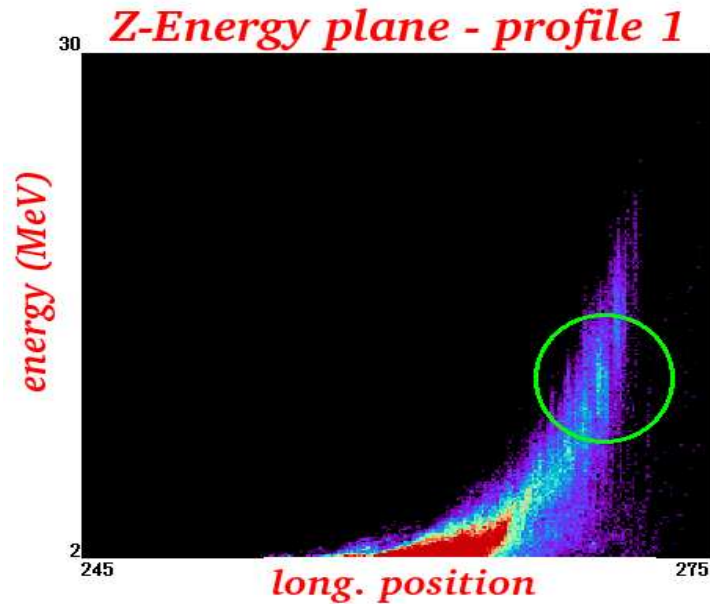
- Density evolution shows growth of a main wake-field structure (see the bubble-like in the **left plot**), rather than a regular plasma wave



↑↑
The “bunch” at the exit of the plasma

⇐ In our case, the much longer pulse duration (65 fs) compared to the ideal bubble-like regime (~ 16 fs), leads to interaction of the accelerated electrons with the the laser pulse itself

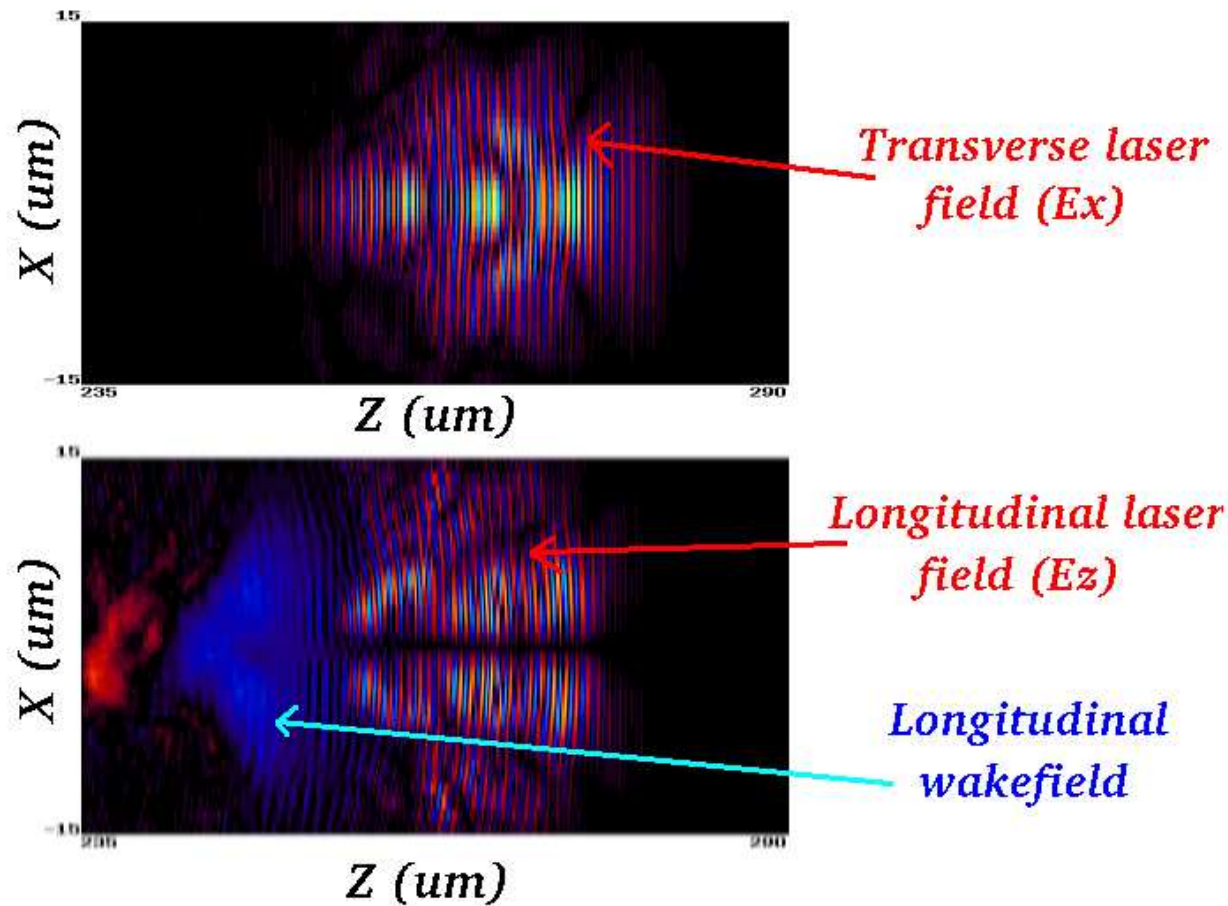
5. Application II: ALaDyn @ PLASMON-X



- The spectrum of the electrons emerging from the interaction region is sensitive to the density profile and exhibits an overall thermal-like spectrum (until ~ 20 MeV) with some clusters at ~ 9 -14 MeV
- Interaction of the electrons with the mm-sized remaining gas will modify the spectral distribution, possibly depleting the lower energy part. This effect is being evaluated.
- The simulated beam divergence (FWHM) is $\sim 11^\circ$ (profile 1) - 14° (profile 2)
- The charge in the bunch is in the range 0.08 nC (profile 1) - 0.2 nC (profile 2)

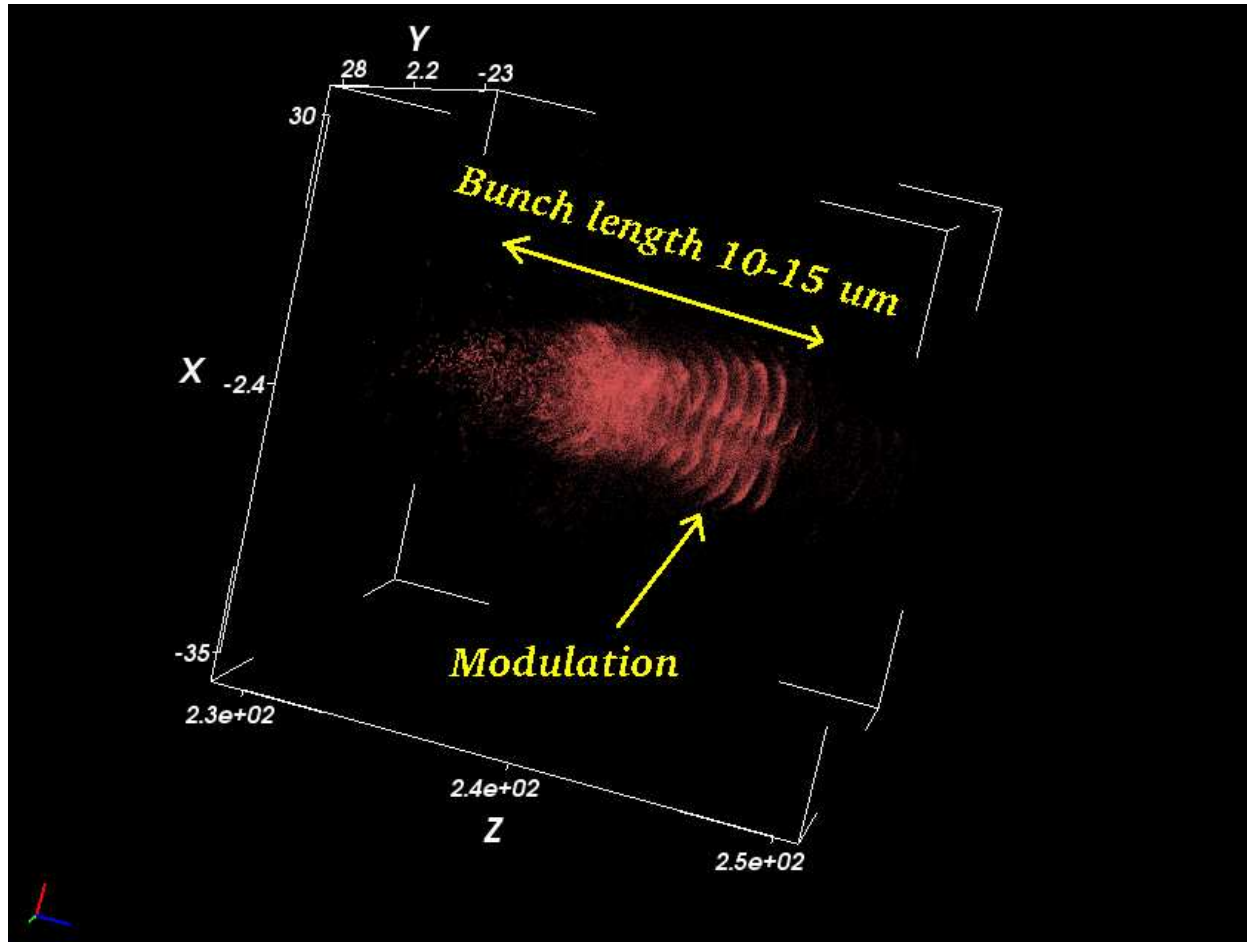
5. Application II: ALaDyn @ PLASMON-X

Modulation of the accelerated electron bunch due to the interaction with the co-propagating laser pulse is an additional source of modification of the energy distribution of the accelerated electrons. This also leads to a modulation of the longitudinal profile of the electron bunch.



5. Application II: ALaDyn @ PLASMON-X

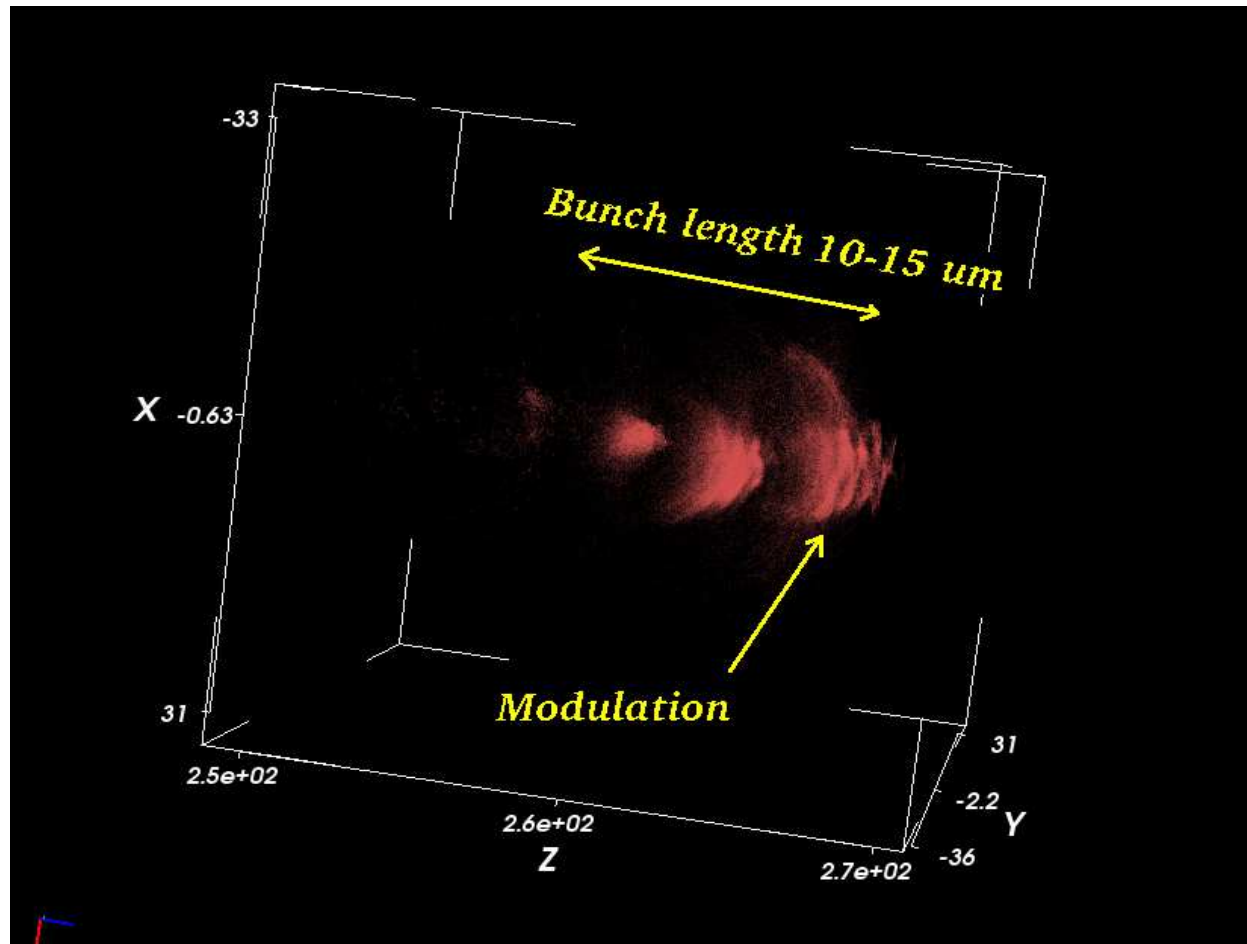
Density profile 1



Modulation of the accelerated electron bunch due to the interaction with the copropagating laser-pulse

5. Application II: ALaDyn @ PLASMON-X

Density profile 2



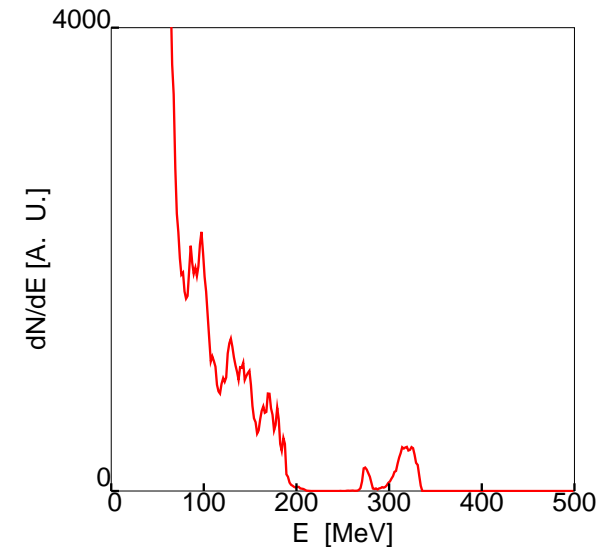
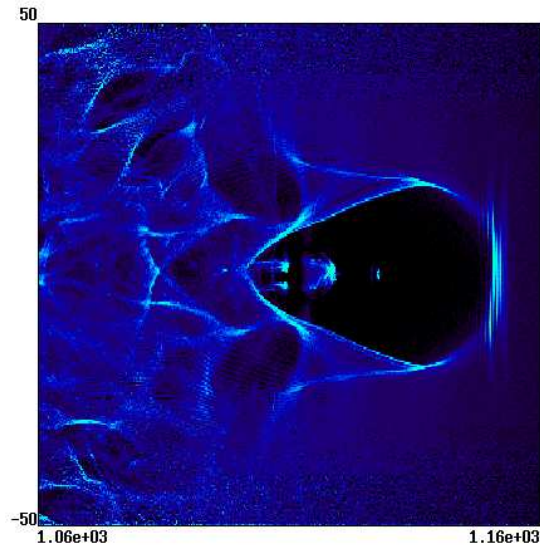
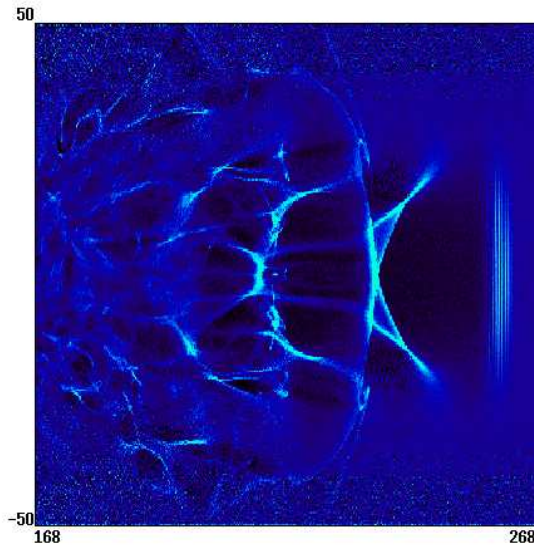
Modulation of the accelerated electron bunch due to the interaction with the copropagating laser-pulse

5. Application II: ALaDyn @ PLASMON-X

Preliminary 2D simulations for FLAME@PLASMON-X (3D foreseen for December 2008)

P [TW]	τ_{FWHM} [fs]
300	20

- simulation: ~ 1 mm gas-jet with $n_e = 0.5 \times 10^{19} \text{ cm}^{-3}$, $I_{laser} \simeq 5 \times 10^{19} \text{ W/cm}^2$



- since ($c\tau_{FWHM} \simeq \lambda_p/2$, $w_0 \sim \lambda_p$) we enter **directly** into the bubble regime without significant pulse evolution
- $E_{peak} \simeq 320 \text{ MeV}$, $\delta E/E \sim 5 \%$, $\epsilon_n \sim 6 \text{ mm mrad}$

6. Conclusions and outlooks

6. Conclusions and outlooks

- A “new” PIC code ([ALaDyn](#)) based on high order schemes has been presented. The code, developed within the framework of the PLASMON-X project, can be “upgraded” in order to meet the user needs (upcoming features: ionization modules, “classical” beam dynamics tracking modules, \dots).
- An application of [ALaDyn](#) to the generation, through LPA, of high brightness e -beams of interest for FEL applications in the contest of the AO-FEL has been presented.
- We have presented 3D simulations of the first “pilot” experiment of the PLASMON-X project concerning LP accelerated electrons and a preliminary study for the 300 TW laser FLAME. Fully 3D simulations are foreseen for December 2008/January 2009.

Thank you!